UiT The Arctic University of Norway

Faculty of Science and Technology

Snow detection on antenna radomes using signal processing

Åse Nordahl Fauske

Master's thesis in Technology and Safety in the High North TEK-3901 June 2022

Abstract

Radomes are dome-shaped covers that protect the antenna from the climate, such as rain, wind, sunlight, and snow. Even though the radomes protect the antenna from snow and ice, it does not prevent snow and ice from building up on the radome. When snow and ice build up enough on the radome, the signal passing through it loses strength. This project tries to detect snow and ice build-up on antenna radomes using the antenna's signal strength and pointing angle. This project has two goals; first is to see if signal processing can be used to detect snow only by looking at the signal strength and pointing angle, and second is to see which analysis tool gives the best results. The data used in this project is the orbital passes of satellites with a signal connection between the antennas and satellites.

The data was first manually classified within the two classes representing the presence of snow or no snow. Then, the analysing tools are applied to the data. The analysing tools used in an attempt to detect the snow and ice build-up are the Fourier Transform and the Linear Discriminant Analysis. First, the Fourier Transform was used to see if the frequency information could be used to distinguish between the classes. Then, the Linear Discriminant Analysis was applied to the data with both the Short Time Fourier Transform and the Fourier Transform. For the last Linear Discriminant Analysis application, the data was segmented.

The classes were not easily distinguished in the frequency domain, but using the Linear Discriminant Analysis and adding descriptive statistics made the difference between the classes was easier to detect. The best results were achieved using the Linear Discriminant Analysis and only looking at a small segment containing the highest elevation angles of each orbital pass.

Acknowledgements

I would like to thank my supervisor, Associate Professor Endre Grimsbø. I would also extend my gratitude to my co-supervisors, Associate Professor Puneet Sharma, and Assistant Professor Per Anton Olsen. Their guidance and feedback have been of great help throughout the project.

Another honourable mention is extended to Stig Kræmer at KSAT for his help getting the project started and providing the materials needed to see it through.

Table of Contents

List of Tables

List of Figures

1 Introduction

The satellite industry has seen exponential growth in the last few years, especially in the number of satellites launched into space. With the introduction of the CubeSat, a small 10 cm3 satellite around the year 2000, the satellite industry changed. It was now possible to launch hundreds of satellites with each launch when the bigger satellite could only be launched one at a time (Chantal Cappelletti, 2020). In addition, the size of the CubeSats dramatically reduced the time and cost of producing satellites, giving many more companies the capability of sending up their own satellites. With the culmination of the increase in launches and the availability of smaller companies sending up their satellites, the need for ground station antennas to communicate with these satellites grew.

The orbiting path varies based on the intended use of the satellite. There are three ways satellites most commonly orbit the earth. First, is a geostationary orbit in which a satellite moves with the earth in such a way that it is always over the same geological position. Second, low earth and medium earth orbit, often in a tilt rotating from west to east around the equator. Third, the polar orbit which moves from north to south, scanning the earth up and down, moving east or west with the earth's rotation. The most common polar-orbiting path for satellites is a sun-synchronised orbit. Sun synchronised orbit is where the satellites move with the sun, always having the sun irradiation to light up the areas the satellite is flying over. (Ippolito, 2008)

For satellites in polar orbit, the best locations for the downlink antennas are in the arctic regions as the satellites for each rotation reach within the line of sight of the antennas in the poles. The rotation of a polar-orbiting, sun-synchronous satellite can be seen in Figure 1. They are called polar orbiting but will always have a slight tilt to the rotational axis, as illustrated in the figure above.

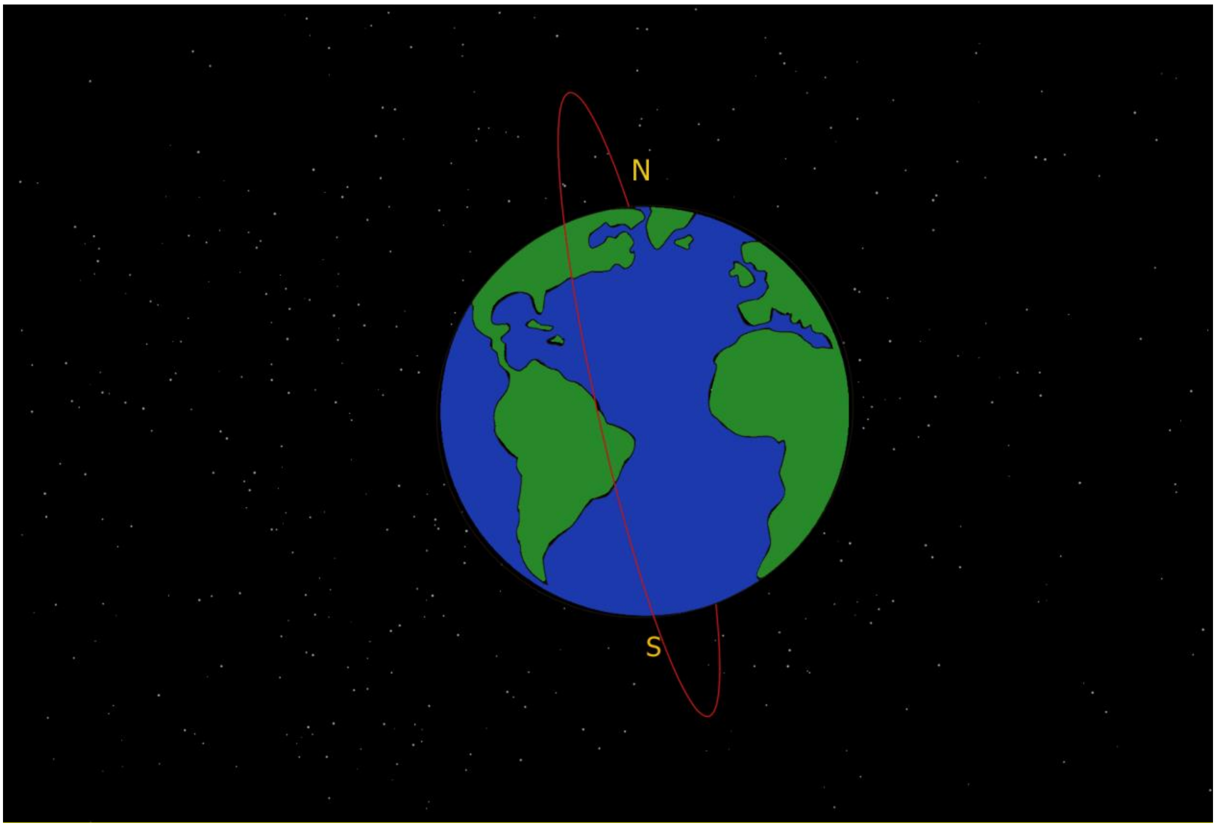

Figure 1. *Polar orbiting satellite orbit illustration*

KSAT is one of the companies within the ground to satellite communication for the earth observation satellites industry. With over a hundred antennas worldwide, they constantly communicate with thousands of satellites monthly. (Anon., 2022) Because most Earth-observing satellites go in a polar orbit, most of KSAT's antennas are in the polar regions. Their largest antenna parks are located within the northern and southern polar circles. These are the Troll research park in the south pole, Troms in north Norway, Inuvik in Canada, and Spitsbergen, the largest Island part of the Svalbard archipelago. The antennas vary from a few meters in height, typically used for smaller satellites, to 20 to 30 meters high, which are used for communicating with larger satellites. They are parabolic-shaped antennas, also known as a dish-antenna, shaped like a bowl that reflects the signal into the middle of the dish where a small rod antenna captures the signal.

The significant challenges with antenna operations in the arctic regions are caused by the climate and general inaccessibility. To protect the antennas from the harsh arctic climate, radomes are used to cover the antenna, reducing wind effects and temperature loss. The radomes also completely shield the antenna from snow build-up, as the antenna's dish shape easily captures the snow. In addition, the radomes have enough room inside of them to let the antenna use the full 360 azimuth degrees and 180 elevation degrees. The azimuth is the horizontal axis the antenna can rotate in, and the elevation is the vertical axis, where it can point from the ground to the sky. An illustration of a satellite antenna with azimuth and elevation angles is shown in Figure 2.

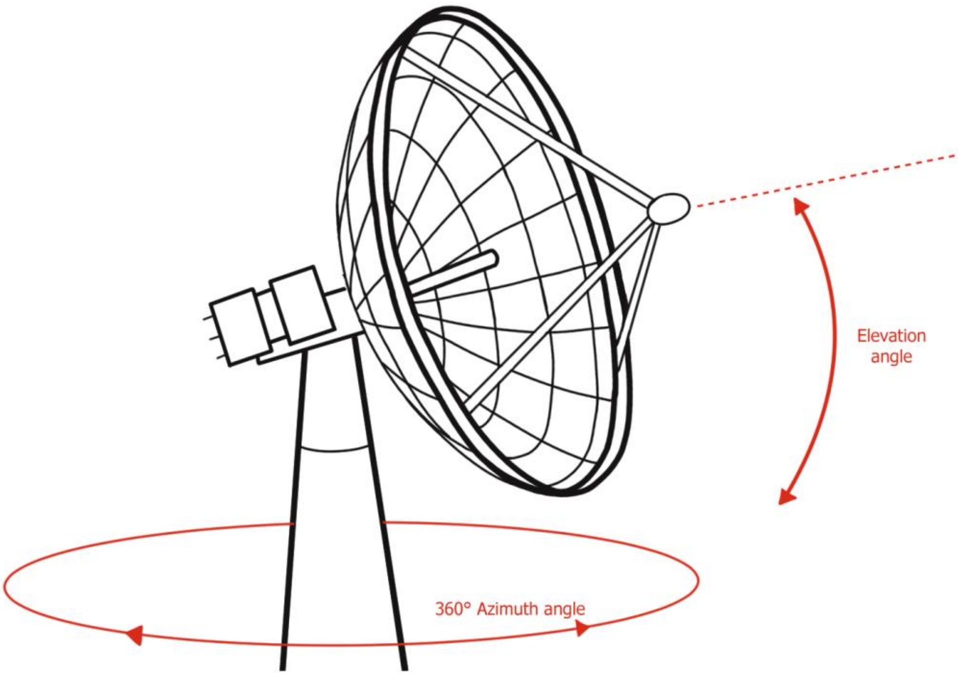

Figure 2. *Satellite antenna with azimuth and elevation angles*

The radome is made from materials that have minimal interference with the electromagnetic signals sent and received from the antenna. Radomes are constructed using self-supporting materials, like fibreglass or a flexible fabric. (Kozakoff, 2009) Because of the extreme weather conditions in the arctic, the former is used on the artic antennas. In the coldest regions, a heating unit is placed inside some of the radomes to stabilise the temperature around the antenna. An image of one of the radomes on Svalbard's station called Svalsat can be seen in Figure 3.

Figure 3. *Svalsat antenna with radome covering (Anon., 2022)*

Even though the radomes are made of a non-sticky material, they get snow or ice build-up. When snow or ice accumulates, the signal sent to and from the antenna gets attenuated. If the snow and ice are not removed, the signal will be weakened when the antenna points in the direction where the snow or ice has accumulated. The snow or ice build-up is removed by manually using a rope to beat the snow off or when needed, and when needed a crane to lift personnel so that the top can be shovelled. Figure 4 illustrates what a heavy snow load on a radome looks like. The angles illustrated in the image show the pointing angles of the antenna for the elevations. Because of the 360° angle of the azimuth, the elevation only gives the angles from 0° at ground level to 90° looking straight up, instead of a 180° angle from ground level to ground level on the other side.

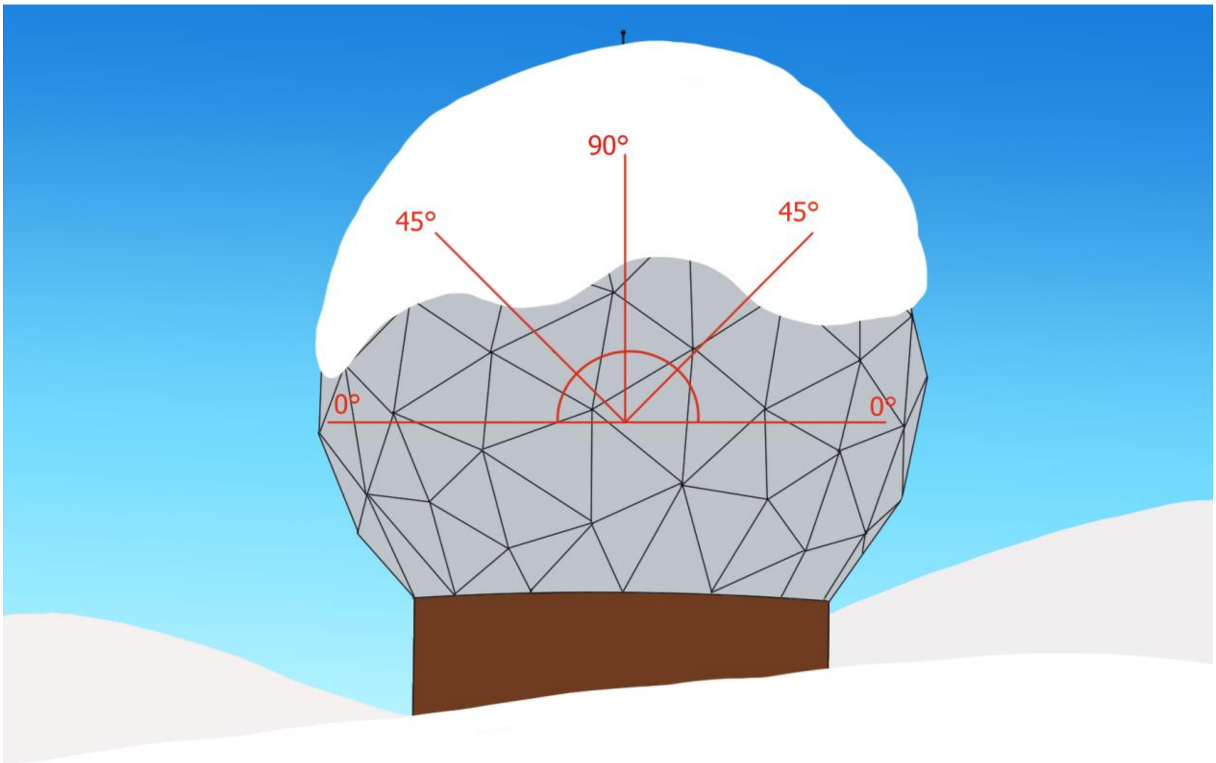

Figure 4. *Illustration of snow on radome and the antennas elevation angles*

KSAT's antennas mainly get signals in X-band and S-band. For this project, the X-band is used due to the relative stability of the signal strength. The X-band is a narrower signal with a frequency of around 7.0 to 11.2 GHz, while S-band has a broader signal with lower frequencies between 2 and 4 GHz. (Elbert, 2008) For a satellite antenna, the S-band communication is primarily used for health data regarding the spacecraft, while X-band communicates the data collected by the satellite. The different uses of the bands are because the X-band signal provides a higher information rate than the S-band.

1.1 Project topic

The antennas are constantly running due to the number of satellites in service, making the need for consistent functionality of the ground operations high. Consistent operations result in snow or ice removal, being an essential task for KSAT's operative ability. Today the snow or ice build-up is removed with a consistent schedule based on the season. When snow and ice have a high accumulation rate, it is often not detected until the satellite owner reports a problem with satellite communication. It can also be detected by the 24 hr operators monitoring the systems when looking at the signal strength and seeing the typical characteristics of snow attenuation.

The goal of KSAT is to make snow detection an automated process, where snow removal will be done on a need basis. The detection is done to have a warning of snow accumulation in time for the personnel to reach the antennas and remove the build-up before the signal strength is greatly affected.

This project aims to answer the following two questions. Firstly, can signal processing be used to detect snow or ice on the radomes, and secondly, which analysis tool will give the highest accuracy of snow detection.

This project uses the signal strength from satellites passing over antennas on Svalbard to detect snow and ice on the antenna radomes. The detection is done by looking for attenuation in the signal strength. KSAT has already gathered the data used in this project, and the parameters will be time, looking angle in both azimuth and elevation and signal strength in X-band.

The project’s end goal is to make a program to automate snow detection, focusing on the accuracy of the snow detection. There will be several signal processing analysing tools used to determine which tool gives the most accurate snow prediction results, applying the analysing tools one by one to find out what has the best prediction results.

2 Theory

2.1 Signals

A signal is defined as a variation in amplitude and frequency over time. One of the most common signals people interact with daily is sound, varying with volume and pitch as a representation of amplitude and frequency. For this project, the signals used will be received signal strength from a satellite to an antenna and the pointing angle of the antenna. These are recorded digitally so that they can be analysed using computer programs. Analogue signals get converted into digital by taking samples of the signal with a constant interval. The signal is converted from digital to analogue because analogue signals have near-infinite samples of frequency and amplitude. To analyse a signal, it needs to be given with known, equally spaced time intervals between each sample.

2.1.1 Project data

The data used in this project is sampled using intervals of one second. For a polar-orbiting satellite, the time it takes to download the information to the antenna ranges from a minute to

15 minutes on average. One satellite moving over the antenna one time is called an orbital pass or a pass for short and will be used for the rest of the paper to talk about each satellite's communication.

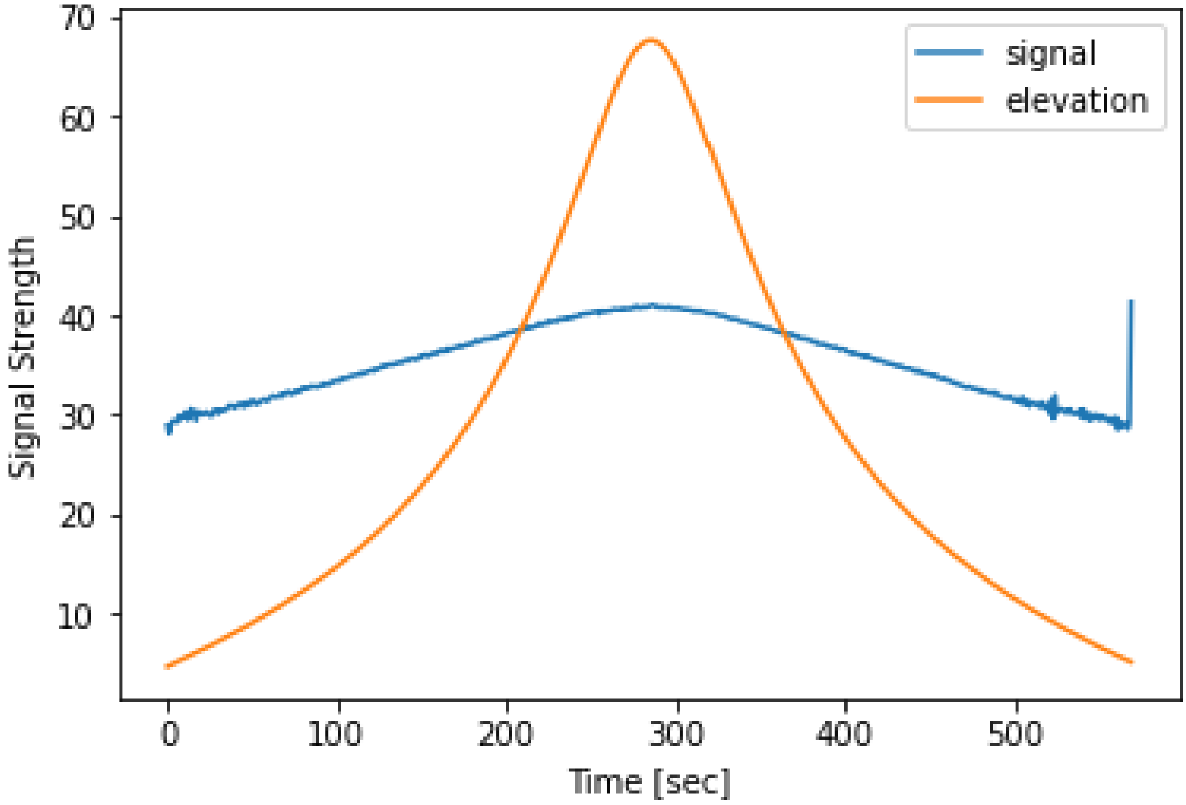

Figure 5*. Signal strength and elevation of a typical satellite pass*

A plot of how generally the data used in this project looks is shown in Figure 5. The antenna usually starts following the satellites a few seconds before it starts communicating with the satellites. This is due to buildings, other antennas or trees near the ground that can interfere with the signal. For most satellite passages, the rule is not to start communicating before the antenna points a few degrees over the ground to avoid interference with ground objects. This example shows a pass with high elevation, reaching 70° at the top. The signal strength changes slightly when the antenna points to a higher elevation. This is due to there being less distance between the satellite and the antenna.

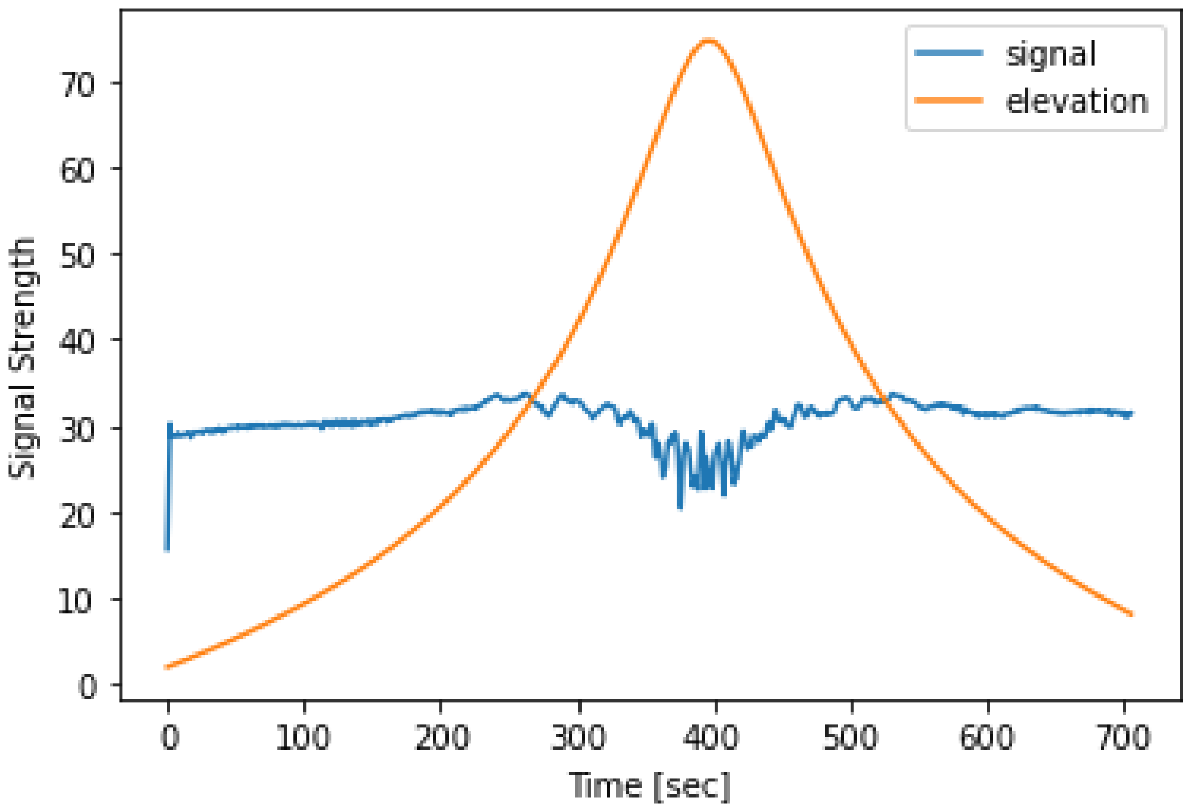

Figure 6. *Signal strength and elevation of a satellite pass with snow at high elevation*

The signal strength will be used to determine if the snow is interfering with the communication by looking for the characteristic attenuation that occurs at high elevations, an example of how this typically looks is shown in Figure 6. The figure shows a plot of how the signal strength will typically be affected by snow. The snow lying on top of the radome typically has more coverage at the top and less toward the sides, making the shape of the signal strength loss a downward pointing curve. Even though the snow mainly lies on the top of the radome, there are multiple ways the snow can build up. The first way is that the snow lies mostly on one side due to wind conditions, another way is that the snow lies more on the sides than the top. The snow coverage can also be uneven distribution because part of the snow has fallen off, affecting how the snow attenuation will appear on the signal strength.

Even though the snow attenuation usually has a characteristic look, several other factors can affect the signal's strength. These will show up as attenuation or total loss of signal. If they occur simultaneously as the signal goes through the snow, they can obscure the shape of the attenuation or indicate that there is snow even when there is not.

Time series signal processing is data processing that varies by time in frequency and amplitude. The frequency is the number of whole sine or cosine waves within a set period, usually defined using Hertz, which has a period of 1 second. The frequency is given as ω, which is the sine or cosine wave per time, written as $\frac{2\pi}{T}$, where T is the time and 2π is the length of one wave. The amplitude is the maximum height of the sine wave compared to the zero line. The data for this kind of signal processing is captured with equally spaced sample periods. The method of transforming a signal given as a function or an infinitely long signal is called a time-continuous transform. The method of transforming a signal that has a finite number of samples is called a discrete transform.

Time-dependent signal processing looks at how the signal changes with respect to time. For this project, there will be two different signal processing techniques used. These are the Fourier Transform and the Short-time Fourier Transform.

2.1.2 Fourier Transform

The method of time-series signal processing that is considered the simplest and most widely used is the Fourier Transform. The Fourier Transform works by transforming the signal from the time domain into the frequency domain. This is done by decomposing the signal using frequency and amplitude. The decomposing works both for infinite signals given as a function and sampled finite signals. The decomposition will represent the signal as sine and cosine waves. For signals transformed using the time-continuous Fourier Transform, the amplitude is defined as the magnitude of the wave, and the frequency is represented as the oscillation. (Kreyszig, 2011)

To show how the signals are decomposed from the time domain into the frequency domain, two sinusoidal waves, one with an amplitude of 5 Hz and another with an amplitude of 10 Hz, are used. The signals are shown in Figure 7. The sum of the two signals is shown in Figure 8. The Fourier Transform of the three signals can be seen in Figure 9. The two signals at the top show the amplitude of 5 Hz for the first and 10 Hz for the second signals. The bottom Fourier Transform shows the frequency of the 5 Hz and 10 Hz as the sum of the signals.

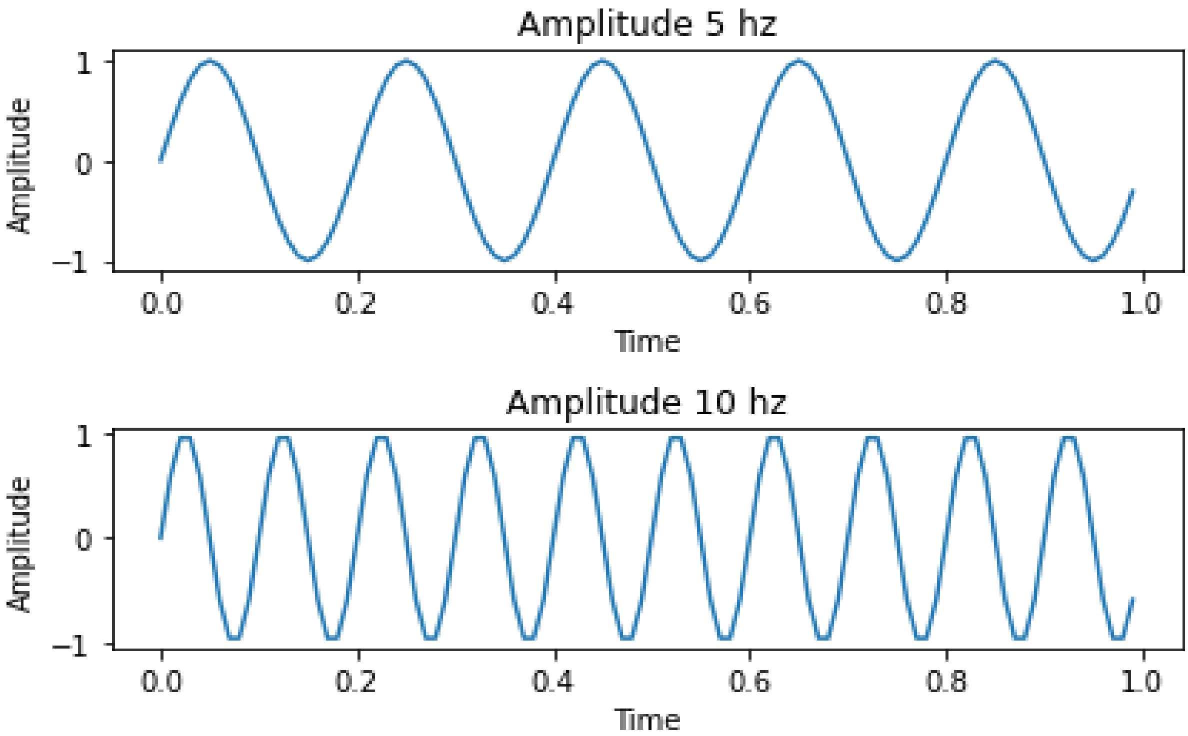

***Figure 7**. A. Sinusoidal waves in 5 Hz and B. 10 Hz amplitude shown in one second*

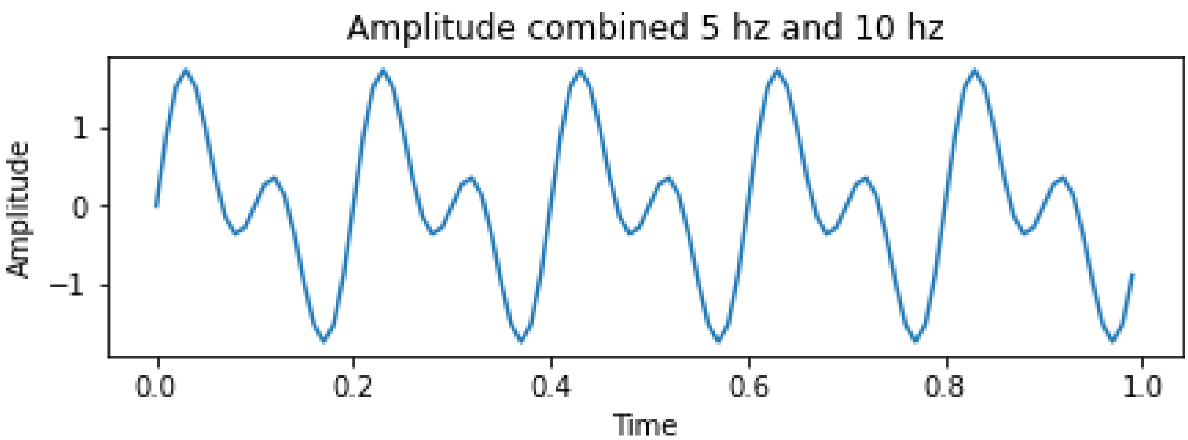

***Figure 8.** Sinusoidal wave sum of two sinusoidal waves with amplitude an of 5 Hz and 10 Hz*

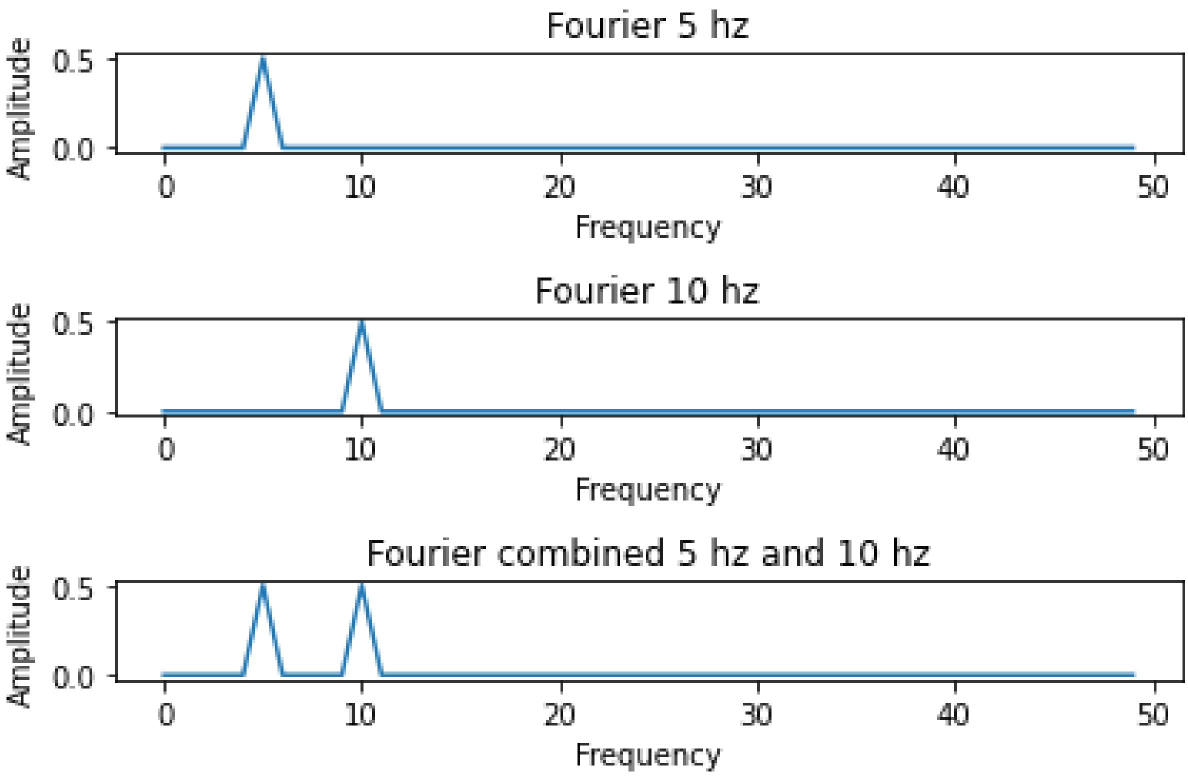

Figure 9. *A. Fourier Transform of sinusoidal waves 5 Hz, B. Fourier Transform of sinusoidal wave 10 Hz and C. Fourier transform of the sum of the 5 and 10 Hz*

The definition of the time-continuous Fourier Transform is given in (2.1).

$$f(k) = \int_{-\infty}^{\infty} f(x) e^{-2\pi i k x} dx \qquad (2.1)$$

The Fourier Transform is given as an infinite integration of the signal using the individual samples x. The Fourier Transformed signal *f(k)* is dependent on the original signal *f(x)*. The original signal is transformed from the time domain to the frequency domain by the integration of the signal times the factor $e^{-2\pi i k x}$. This factor is based on Euler's formula, which says that a complex sinusoidal function can be written as the exponential of the imaginary times the signal samples, as shown in (2.2).

$$e^{ix} = \cos x + i \sin x \qquad (2.2)$$

Within the factor, the signal is multiplied by the number of samples k and the period of one signal 2π. It can also be written as $e^{-\omega i x}$ as ω is equal to the frequency of the signal.

Because the time-continuous Fourier Transform is infinite, it only takes in functions or infinite signals, making it inapplicable to real signals, as real signals are discrete, recorded with a start and a finish. The Discrete Fourier Transform (DFT) is used to apply the Fourier Transform on real signals. The definition of discrete is something that is individually separate and distinct. Taking in *n* number of samples from a signal, each sample is represented as *x*. Doing the same as the time-continues Fourier Transform by transforming the signal into sine and cosine, only for a defined number of samples *N*. The DFT requires the signal to have equally spaced samples. The equation for the DFT is shown in (2. 3).

$$f_k = \sum_{0}^{N-1} x_n e^{\frac{-2\pi ikn}{N}} \qquad (2.3)$$

The fastest and most widely applied use of the DFT on a dataset is the Fast Fourier Transform (FFT). (Cochran & Cooley, 1967) This is an efficient procedure that takes advantage of the fact that the calculation of the coefficients of the DFT can be carried out iteratively. This saves considerable computation time without changing the result. The FFT also has the additional benefit of reducing round-off error that can occur with the Fourier Transform computation.

The strength of the Fourier Transform is its ability to display the whole signal as an infinite sum of complex sinusoidal functions. Allowing the signal to be broken down into its fundamental components. The biggest drawback of the Fourier Transform is its inability to tell where the different frequency components are located in the time-varying signal. It only tells that the different frequency component exists somewhere within the signal. This will affect the level of analysis that can be applied to the results of a time-varying signal.

2.1.3 Short-time Fourier Transform

The biggest disadvantage of using the Fourier Transform on a time-variant signal is that it will not show when the different frequencies are present in the signal. Knowing the time location of the frequencies is important if the properties of interest are located at a specific time within the signal. The way to solve this problem is by using the Fourier Transform in smaller windows to get a time and frequency location for each window.

The Fourier Transform can be used to display information in the frequency domain with information from the time domain by using the Short-time Fourier Transform (STFT). The STFT is the product of a sequence of Fourier Transforms of a windowed signal. A windowed signal is an extracted part of a signal that has a given width, this window is moved across the signal, either with a given overlap of each segment or without any overlapping samples. The STFT provides the time-localized frequency information for the signal, this is used where frequency components of a signal vary over time. (Portnoff, 1980) The result of the STFT is given in a spectrogram of frequency and time. This spectrogram is an intensity plot of STFT magnitude over time. This time is dependent on the window size, not the time from the signal in the time domain. Smaller windows in the time domain give better resolution in the frequency domain. The equation for the STFT is shown in (2. 4).

$$X_m(\omega) = \sum_{-\infty}^{\infty} x(n)\omega(n - mR)e^{-j\omega n} \qquad (2.4)$$

$$= DTFT_{\omega}(x \cdot SHIFTmR(\omega))$$

Where the variables are shown underneath.

$$x(n) = input\ signal\ at\ time\ n$$

$$\omega(n) = length\ M\ window\ function$$

$$X_m(\omega) = DTFT\ of\ windowed\ data\ centered\ aorundt\ time\ mR$$

$$R = hop\ size, gieven\ in\ samples, between\ successive\ DTFTs$$

An example of a window function used for the STFT is the Hamming, the function in the time domain is shown in (2.5). (Harris, 1987)

$$h(n) = \alpha + (10 - \alpha)\cos\left[\left(\frac{2\pi}{N}\right)n\right] \qquad (2.5)$$

The width of the window will change the resolution in time and frequency. When the window is narrower, the time resolution increases, but at the same time, the frequency resolution gets decreased. An example of the Hamming window in both time and frequency is shown in Figure 10.

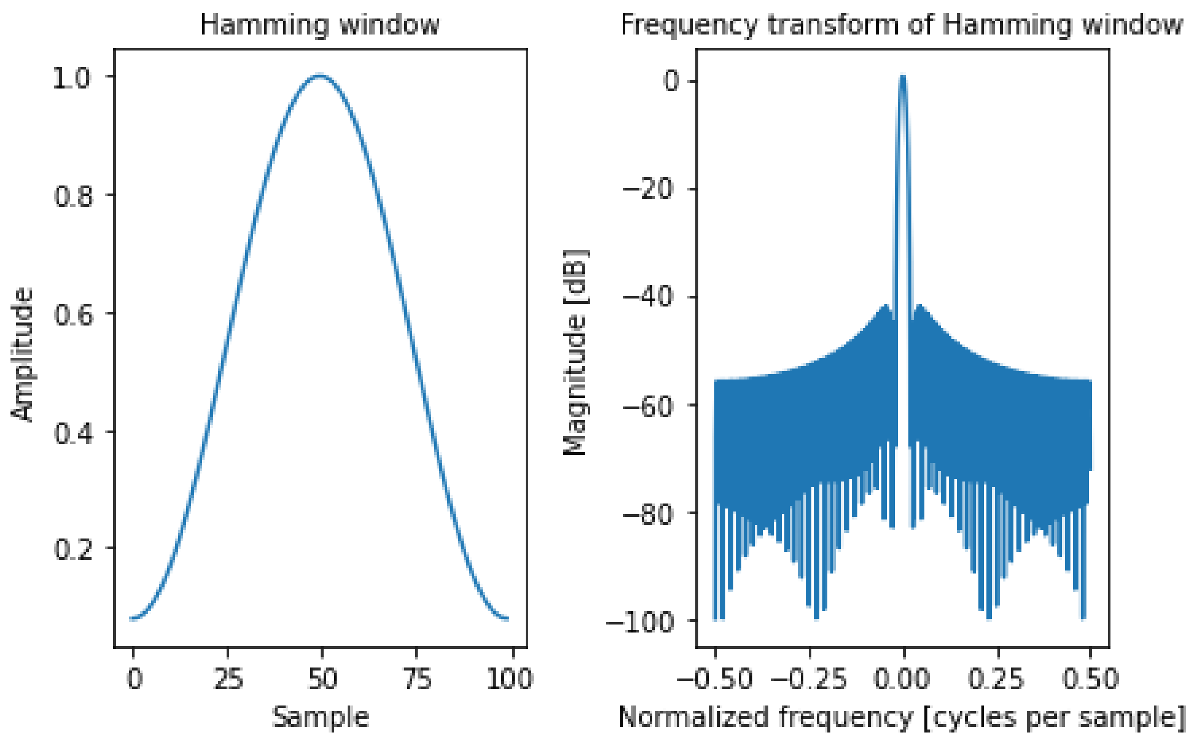

Figure 10. *A. Hamming window in time domain and B. Hamming window in the frequency domain*

Figure 11 illustrates how the STFT represents a signal from the time domain to a magnitude spectrum of the time and frequency domain. The signal used is a chirp, with a frequency from 10 Hz to 100 Hz. A chirp is a sinusoidal signal that gets a higher frequency over time. The signal has 1000 samples, and the window used in the STFT is of size 150. This gets represented in the magnitude spectrum as an almost linear increase from 10 Hz to 100 Hz.

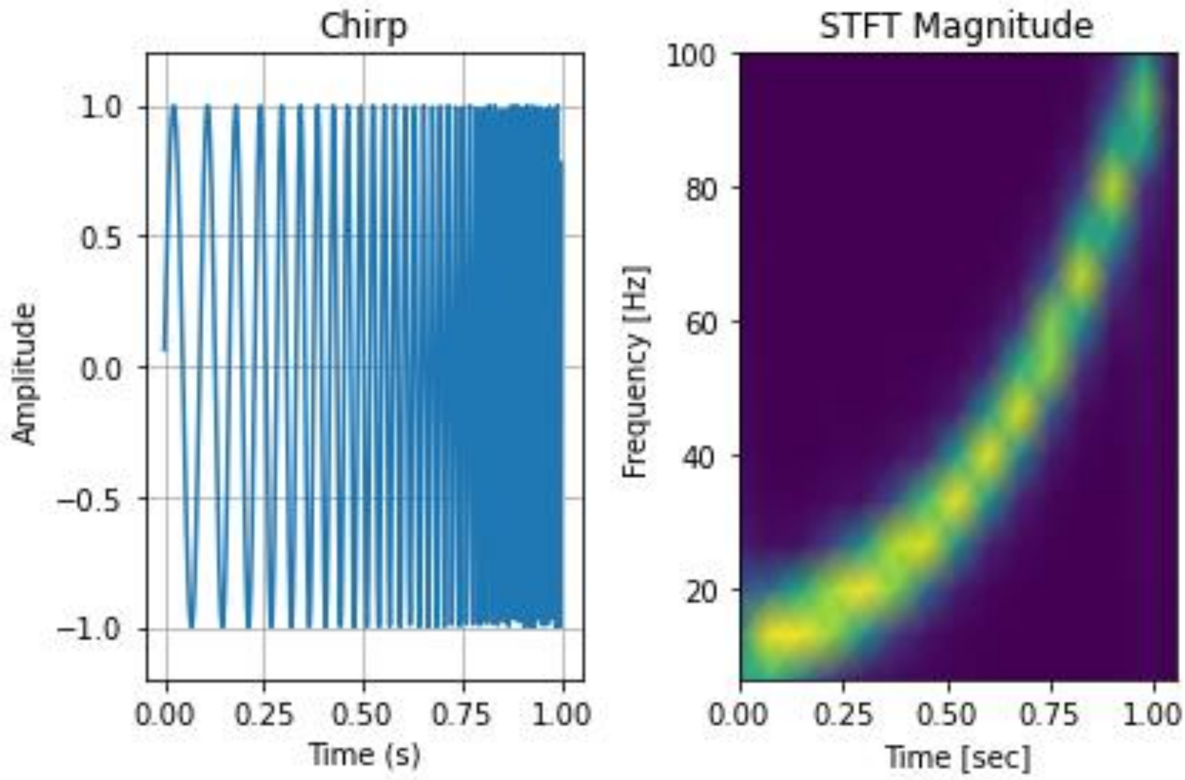

Figure 11. *A. Time representation of a chirp and B. STFT frequency representation of a chirp*

The most significant benefit of the STFT is that it gives both a representation of the local time and frequency content of the signal looked at. This is useful when the position in the time domain of the different frequencies gives essential information. The window function used for the STFT is also of a fixed size, making patterns of consistent sizes easy to spot. When looking at longer signals, the STFT allows the frequency information of each window to not be affected by any of the rest of the signal.

2.2 Linear Discriminant Analysis LDA

Linear discriminant Analysis (LDA) is a dimensional reduction method. It takes in a dataset labelled with two or more classes to reduce the data's dimensions while maximising the separation of the classes. (Xanthopoulos, et al., 2013) This method helps separate multidimensional classified data where the separation of the classes is difficult in the given dimensions. This method is often used to dimensionally reduce data before being fed to a machine learning algorithm. The LDA data can also be used as a model to predict new data with the same dimensions as the original data. A similar method often used to reduce dimensions in datasets is Principal component analysis (PCA), the main difference between the two methods is that the PCA is unsupervised, meaning the data used is not labelled, while LDA takes in pre-labelled data, making the method supervised. (Alsberg, n.d.)

The LDA works by using two different criteria to decide how the dimensional reduction will maximise the category separation. The first criterion is that it will maximise the distance between the means of each category in the new axis. The second criterion minimises the variance within each category in the new axis. The first criterion is achieved using the between-class variation, the equation is shown in (2.6).

$$S_b = \sum_{i=1}^{c} N_i(\bar{X}_i - \bar{X})(\bar{X}_i - \bar{X})^T \tag{2.6}$$

This equation takes the sum of all the classes c, with the sample size N per class and takes the difference between the mean of each class and the mean of all classes. The second criterion is achieved using the within-class variation, the equation is shown in (2.7).

$$S_w = \sum_{i=1}^{c} \sum_{j=1}^{N_i} (x_{i,j} - \bar{X}_i)(x_{i,j} - \bar{X}_i)^T \tag{2.7}$$

This equation takes the sum of all classes, and within all classes, it takes the sum of the class's sample size and the value of each sample within the class compared to the mean of the class. (Izenman, 2008)

To show how the LDA works, an example is shown using the Iris dataset. (Fisher, 1936) The three classes of Irises, Iris Setosa, Iris Versicolour and Iris Virginica, are labelled and shown in Figure 12. For this example, only two attributes are used, the petal length and petal width. The Result of the LDA is shown in Figure 13. The aforementioned factors decide the angle at which the data is projected into one-dimensional space to maximise the spread of the classes and minimise the distance within the classes.

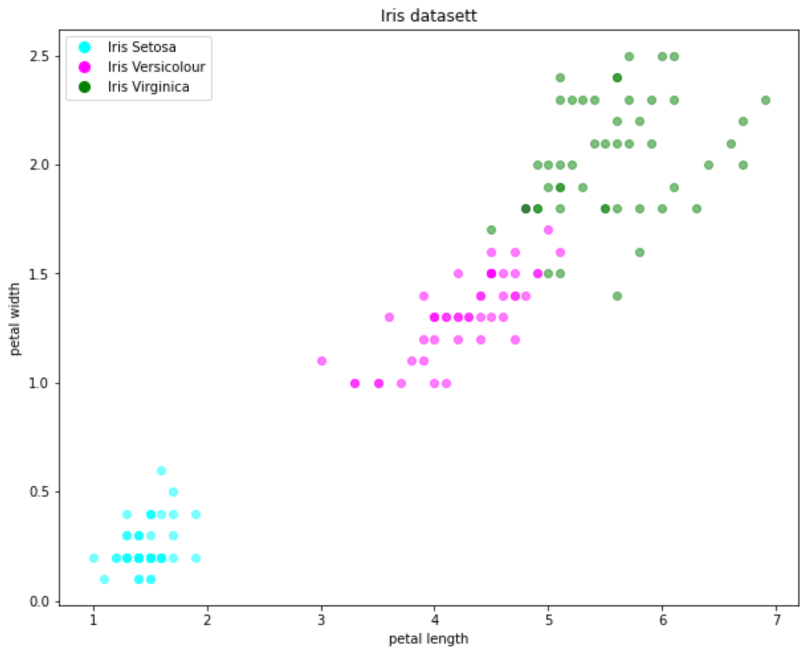

Figure 12. *Iris dataset, three classes of the flower represented by the petal length and petal width*

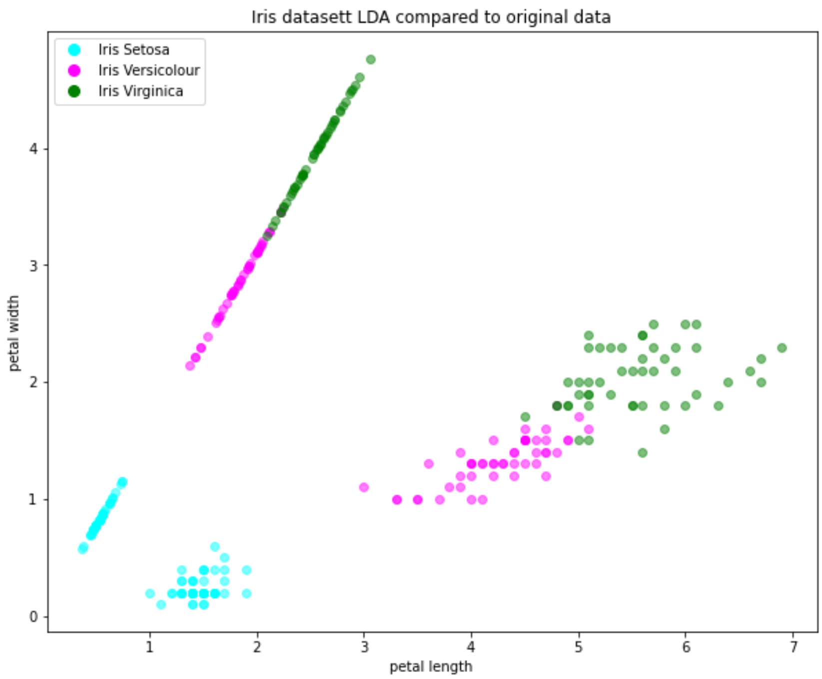

Figure 13. *Iris dataset LDA projection compared to original data*

One of the benefits of using the LDA is that the dimensionally reduced data can be used to categorise new data. A new set of data with the same original dimensions can be fitted into the original data to determine its classification, using the same reduction parameters as the original data. Making LDA applicable as a prediction model. For projects with data with multiple dimensions and classes that are not easily differentiated, the LDA will help clarify the differences between the classes while reducing the dataset's dimensions.

3 Methods

The data used in this project are signal strength, elevation angles, and azimuth angles taken from antennas on Svalbard between September and May. This data contains only passes connected to the satellite, with a downlink in the X-band received from the big antennas. These antennas have two main ways of writing signal strength. One of the antennas gives a number based on an established zero value. In contrast, the other gives a seemingly more arbitrary number, varying with the antenna. To have the data as similar as possible only data from the first type of antenna is used.

The project will do two separate data analyses. The first is pre-processing, where the data will be sorted into separate passes that can later be analysed. A selected part of the datasets will be manually classified during the pre-processing. The second analysis will be the application of signal processing. Here the two main analysing tools applied are the Fourier Transform and the LDA. These tools are used to see if there is any way to classify the data into two classes, snow or no snow. This project uses Python as the primary programming language for all the analyses.

The main libraries used for the Python programming in this project are shown in Table 1.

Table 1. *Main libraries used in Python*

Method	Library
Fourier Transform	Scipy
Short-Time Fourier Transform	Scipy
Linear Discriminant Analysis	Sklearn
Test Train split	Sklearn

3.1 Pre-processing

The raw data is sorted and pre-processed to get a dataset that will be easily analysed and has relevant data. However, only a small part of the data will be chosen for the signal processing analysis. The small dataset is chosen to represent a variety of the way the data presents itself while being small enough for manual labelling.

The raw data is presented as a long column of every sample from every pass from each antenna. The data is received from ten antennas, labelled in this project as 1-10. The time, tracking ID, azimuth angle, elevation angle and signal strength from the X-band are given for each sample.

Using the tracking ID, each pass is separated into a new column. This separation allows the signal processing to look at each pass separately.

After the separation, the maximum elevation angles of each pass are used to filter out the relevant data. The radome shape causes the snow to lay on the crown of the radome. Because of this, the project only uses passes that reach 45° or higher in elevation angle.

The first sample size is 200 passes, where 20 passes are chosen from each of the ten antennas., The passes are manually labelled between the two classes, snow or no snow, to compare the results to a solution. The classes are represented as binary 0 and 1, where 0 is no snow and 1 is snow. The label of snow was only given to passes with moderate to severe attenuation of the signal strength. Because of the difference in signal strength between the passes, the attenuation at which the signal strength is impacted severely to moderately is determined based on the distance between the signal strength and the zero floor. The labelling was done by someone with extensive knowledge of signal strength analysis and can be considered an accurate label.

A five-point moving average was applied to the signal. The moving average was applied to try and lessen the effects of peaks and dips in the signal. However, the moving average did not improve the noise in the passes significantly enough to be used further.

A manual edge detection method was applied to try and remove the beginning or end of some of the passes. The edge detection is done because some of the beginnings and endings of the passes have several data points where the signal strength is at its zero floors. This edge detection method removed some of the zero-floor data. However, due to the data's gradual increase from the zero-floor to the signal detected, it was only partially successful in removing them. In addition, many signal strength spikes within the signal also caused a problem with edge removal. A better method would be an edge detection filter where the size is adjusted to give the best removal without affecting the rest of the signal.

3.1.1 LDA pre-processing

The sample size used for the LDA model was increased to 1000, taking 100 passes from each of the ten antennas. All the passes had a maximum elevation higher than 45°. Increasing the number of passes used to make the LDA model will give the model the ability to predict a broader range of passes. This is due to an increase in the number of passes resulting in an increase in the representation of ways the passes look. In addition, all the passes were manually classified as either attenuated by snow or not attenuated by snow.

Several groups of passes were removed to make the passes as uniform as possible to decrease noise and other factors that would impact the frequency representation of the passes. The first thing that was done was to look at consistency in how the signal strength is presented. Looking at each antenna's dataset, one antenna had a significantly different signal strength representation and was decided not to be used further in the project. All the signals were the X-band signal were recorded, but no connection was made to the spacecraft were removed, as they would not give any information on whether there was snow on the radome or not. Any signals where the elevation recorded moved in jumps or stood still for any moment were also removed. The last group removed are passes with a length shorter than 50 samples, as anything under that would likely not show any difference in the classifications.

For the LDA to make a good prediction model, the number of passes within each class should be the same. To ensure that one of the categories does not outweigh the other, the number of passes in each class was made equal. The smallest class dictated how many passes there could be from each class. Here the smallest class is the snow class, with 142 passes. A few unsuitable passes were removed, making the number of passes taken from each class 139. The passes from the other class were randomly chosen to ensure a broader view of passes. The total number of passes used for the LDA ended up being 278.

3.2 Signal processing

The signal processing part of the project has two main analysing tools, with the last tool being applied with three different input data sets looking at different features. The first tool uses the

Fourier Transform to get the frequency information of each pass. The frequency information is used to determine the difference between the classes. The mean of each class is calculated and compared to find the difference. The second primary tool is the LDA, the LDA is used as a prediction model. The first LDA model takes in the STFT information of the passes as well as descriptive statistics of the passes in the time domain. The second LDA model segments the passes into equally sized segments, each with the same class as the whole pass. This model takes in the Frequency information using the Fourier Transform and the descriptive statistics of the time domain data. The third LDA model only uses one segment from each pass. The segment used is the segment containing the highest elevation from each pass. This model also takes in the frequency information and descriptive statistics from the time domain.

3.2.1 Fourier Transform

For this project, the Fourier Transform used is the FFT. First, the Fourier Transform is applied to the data, taking the absolute value of the FFT to make a power spectrum showing the amplitude of each of the frequencies represented in the data. Then, the zero component is removed to normalise the data by subtracting the signal strength's mean from each signal strength sample.

The frequency data is used to make an average plot of each of the classes. The average plots also include all the passes used to make it, showing the variation in the representation of the frequency data for each class. The variance between the mean and the passes used to make the mean is represented as a plot, showing the variation in amplitude for each frequency. The difference between the averages are shown by plotting them together.

3.2.2 LDA with STFT

The LDA uses the data sorted and labelled in the pre-processing for LDA. The STFT is taken for every pass, removing the imaginary part by taking the absolute value of the STFT. The STFT is applied using a Hann window with a window size of 50 samples with no overlapping between windows. The STFT gives an array with 26 samples in 10 to 30 frequencies based on the pass length. Because of the length difference between the STFT result for each pass, only the first 26 samples are used in the LDA, as the first frequency often has the most information.

The LDA takes the STFT and eight different descriptive statistics from the time domain. The descriptive statistics used are the mean, median, variance, standard deviation, kurtosis, skewness, and median elevation. To verify the LDA model, the data is split into two groups, test data and train data, using a test train split. Each group contains the passes and their corresponding labels. The testing and training data allow the LDA to test the accuracy of the classification model. For this project, the testing size was set to 40% of the passes, and the training size was 60% of the passes. The result is an accuracy score, showing how much of the test data was correctly classified based on the labels.

The accuracy score gives an image of how well the classifier works. The accuracy score is given by comparing the model labels of the test data to the labels they have from the manual labelling. The accuracy score is used as the primary way the models are evaluated.

3.2.3 LDA with Fourier Transform

Because the frequency information depends on the pass length, the only way to maintain all the information is by making each pass equally long. Removing frequency information will result in a lot of information loss, so instead, each pass is segmented into segments of size 50. The size is chosen because the snow usually covers about 50 samples. For passes that cannot be divided into segments of size 50, the residual samples are removed equally from the beginning and the end of the pass. For cases with an odd number of samples left, one more is removed from the beginning than the end. The removal is done at the beginning and end because that area often has noise from connecting or disconnecting with the spacecraft. All the data related to the pass is maintained when splitting into segments, and each segment has the same classification as the whole pass. Segmenting the data increases the data size used for the LDA about eightfold.

The Fourier Transform's absolute value is calculated from each segment's signal strength. Therefore, when the segments are the same lengths, the frequency data for each segment will be the same length. This will allow all the information to be retained when implementing the LDA.

The LDA takes in the frequency information from the Fourier Transform and eight different descriptive statistics from the time domain of each pass. The descriptive statistics are the mean, median, variance, standard deviation, kurtosis, skewness, and median elevation. When using the FFT, the segment's frequency information length is 25 samples long. The data is split between the testing and training datasets. The testing size is 40% of the passes, and the training size is 60% of the passes.

After looking at the results, another descriptive statistic was added. This was the distance in height from the pass's maximum elevation to the segment's mean elevation.

To assess how the variables put into the LDA impact the accuracy scores, each was removed one by one to see how the accuracy score changed when each was not included.

A matrix of all possible combinations of the variables was made to get a better image of how the accuracy changes with the variables. The LDA was run with each variable variation to determine how the accuracy changes with the variables. This will also show the variable variations with the highest accuracies.

3.2.3.1 LDA with the highest elevation segment

The last implementation of the LDA is done with only one segment from each pass. The segment is taken from the segmentation previously done. Because the snow mainly lies on the crown of the radome, the highest elevations would be the most important area to look at to identify if there is snow. Unfortunately, the passes are often not centred with the highest elevation in the middle. Some passes only have an increase or decrease in elevation, placing the highest elevation at eighter of the end. This makes trying to centre the segment around the highest elevation difficult. Therefore, the segment is taken from the previous segmented passes and chosen based on which segment contains the highest elevation angle. This results in the segments having the highest elevation anywhere within it and not consistently centred at the middle of the segment.

The LDA uses the frequency information from the Fourier Transform and the same descriptive statistics as the previous LDA method, except for the distance between the maximum elevation and the mean elevation of the segment.

The segments ' window size was adjusted to see how the LDA model's accuracy changes. The segment sizes were adjusted from 30 samples to 150 samples with increments of 10. Each variable was removed one by one for each window size to determine which window size gave the best overall accuracy. Then, looking at the accuracy score for each window size compared to the accuracy score with the different variables removed, one window size was chosen with the best overall accuracy score. The same matrix of variable combinations was used as the previous LDA model to find the variable variations with the highest accuracy score.

The test train split was changed to verify the top results of the matrix and window size for the LDA model. The test train split was applied in ten different ways to choose which passes were the training set and the testing set. This was done to see how the difference in passes chosen would impact the accuracy score. The variable variations chosen to verify were the ones with the 20 highest accuracy scores. The mean and variance of each variable variations results were also recorded. The variance within the results shows how consistent the results are with the variable variations, and the mean shows the overall accuracy of each variable variation.

4 Results

4.1 Fourier Transform

When looking at the power spectrum from the Fourier Transform of the passes, it generally follows an exponential shape. One example of the frequency representation of the signal in the time domain is shown in Figure 14. Part A of the figure displays the signal strength and elevation in the time domain, while part B shows the power spectrum from the Fourier Transform. Most of the frequency information is located between 0 Hz and 0.1 Hz. Looking at the difference between passes with and without snow, there is a general trend where the higher frequencies reach low amplitude faster when there is less snow attenuating the signals strength. Looking into this further, the more noise a pass has, the more amplitude, the higher frequencies have. This points to a correlation between higher frequencies and noise, not higher frequencies and snow. The more snow is between the antenna and the spacecraft, the more noise the signal strength has, but noise is not exclusive to the areas with snow.

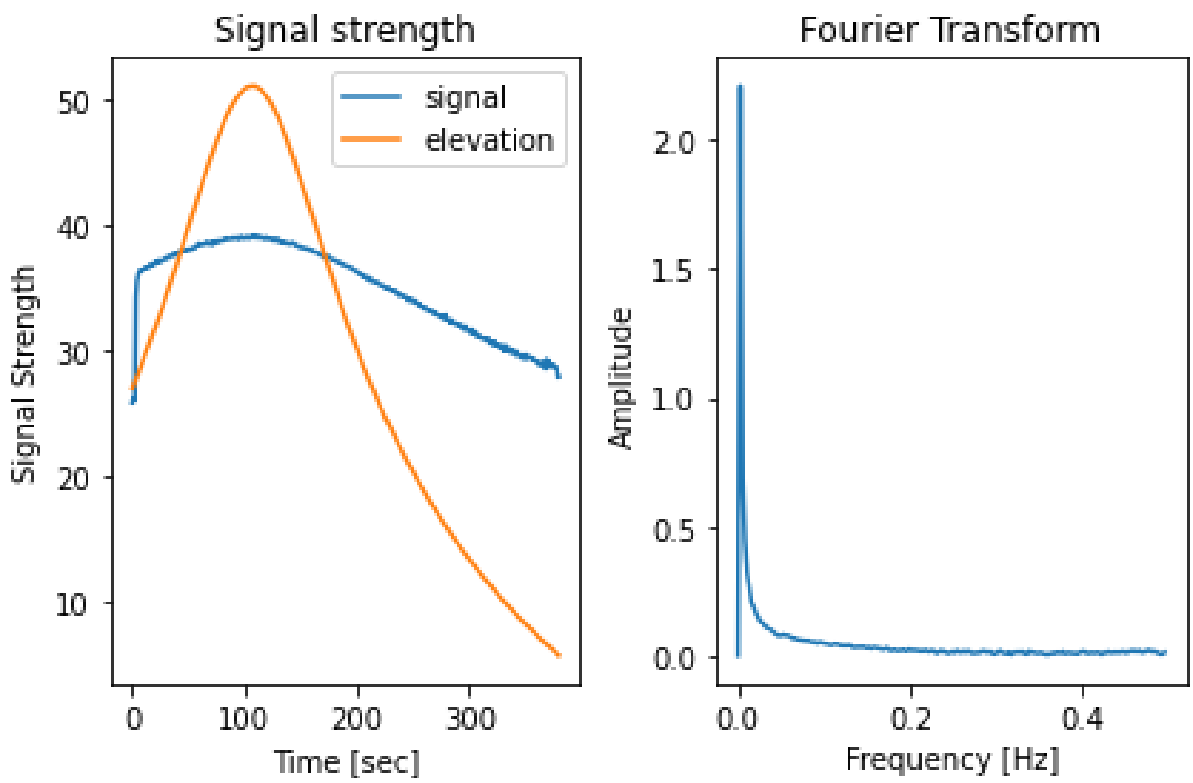

Figure 14. *A. Signal strength of a pass and B. Fourier Transform of the same pass*

Looking at individual passes, the difference in the frequency domain between the classes was not noticeable. Noise and other factors occurring within the pass impacted the frequency information more than the snow attenuation did.

The results of taking the mean of all passes classified without snow are presented in Figure 15. This image shows both the mean and all the individual passes the mean is constructed from. In addition, the image shows the variation within the passes, displaying how much the frequency representations can differ. The line from the zero frequency to the first frequency from each pass is well represented in this figure, as most passes have the first frequency at 0.001 Hz to 0.002 Hz. The variance of each frequency between the mean and the rest of the passes is shown in Figure 16.

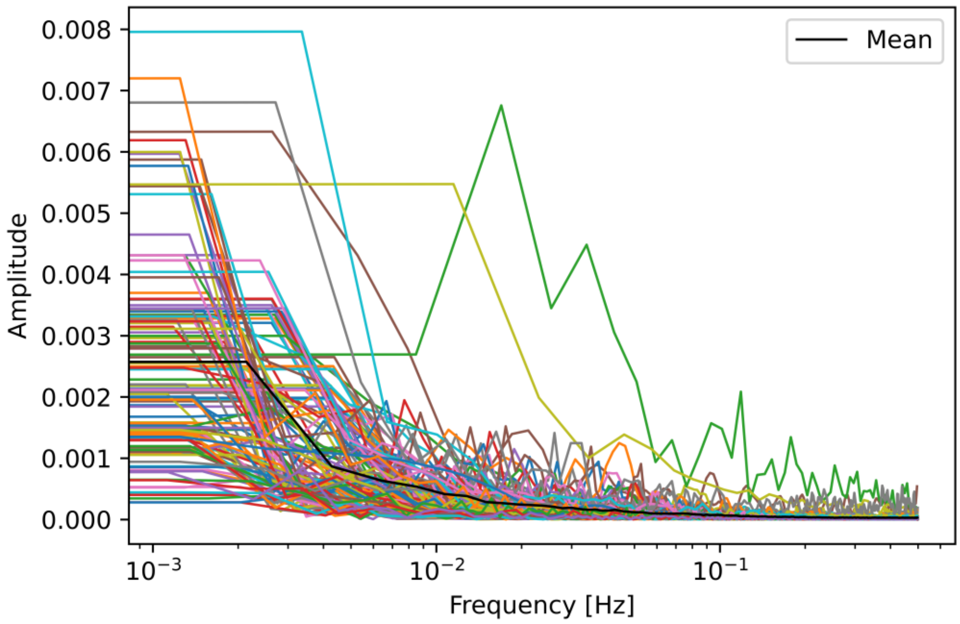

Figure 15. *Logarithmic representation of the mean Fourier Transform of not snow passes represented with the passes that makes the mean*

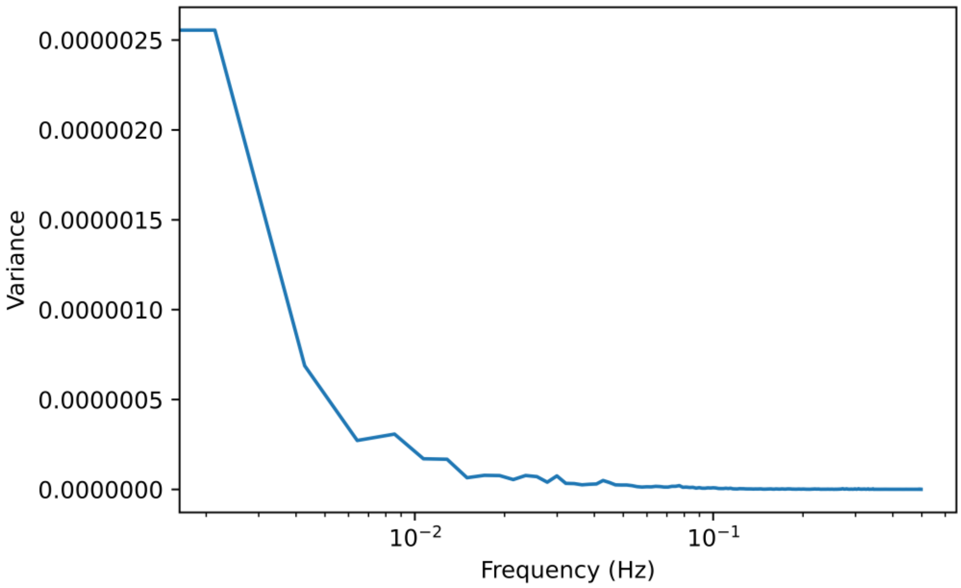

Figure 16. *Logarithmic representation of the variance of mean Fourier Transform of not snow passes*

The mean of the passes with the classification of snow can be seen in Figure 17. One important thing when looking at the mean of this class is that the number of passes in this class is a lot smaller than in the class representing the passes without snow. This results in a less broad view of the pass shapes. The variance of each of the frequencies between the mean and the passes are shown in Figure 18.

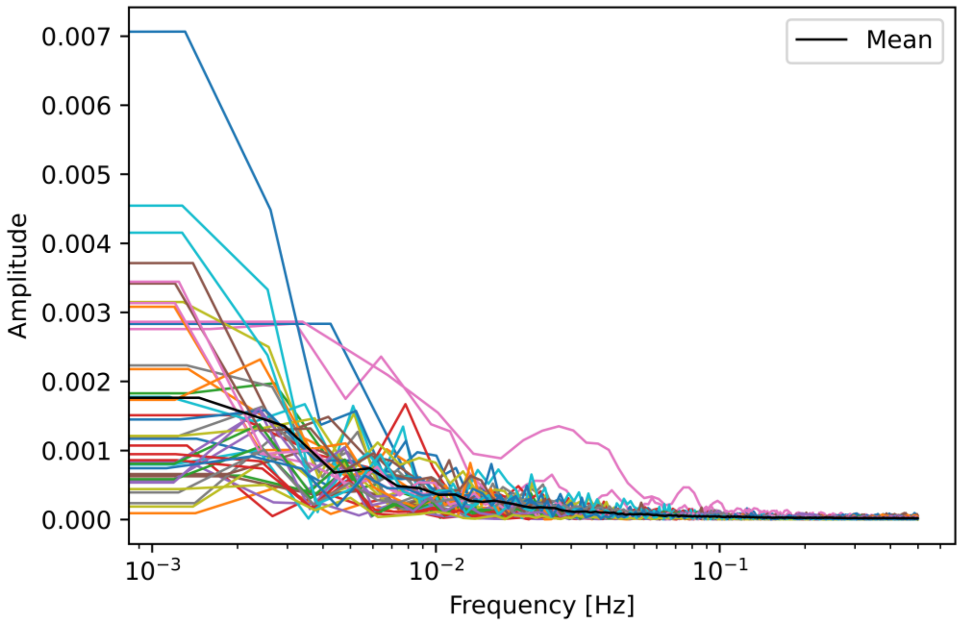

Figure 17. *Logarithmic representation of the mean Fourier Transform of snow passes represented with the passes that makes the mean*

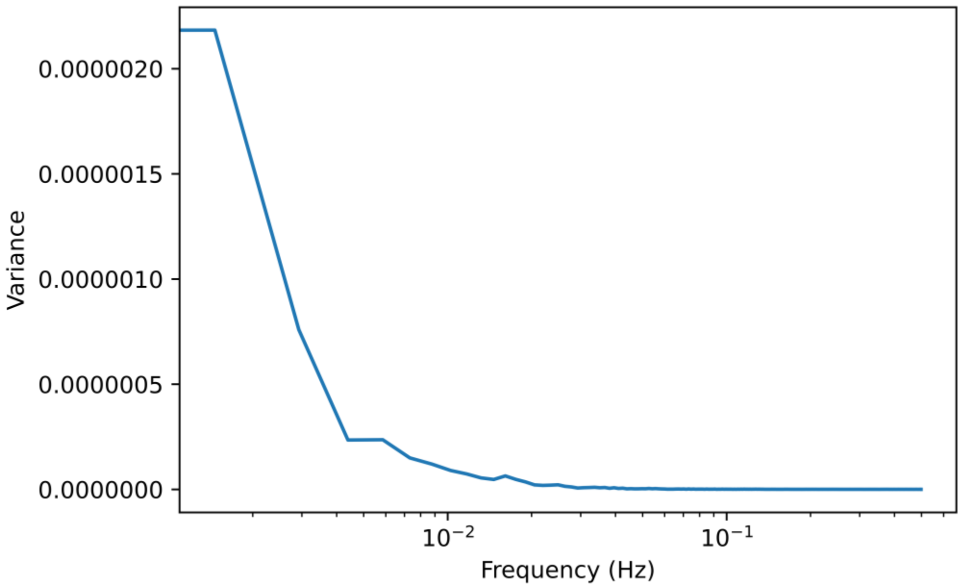

Figure 18*. Logarithmic representation of variance of mean Fourier Transform of snow passes*

The plot comparing the mean of each of the classes to see if any frequencies can tell which class a pass belongs to is seen in Figure 19.

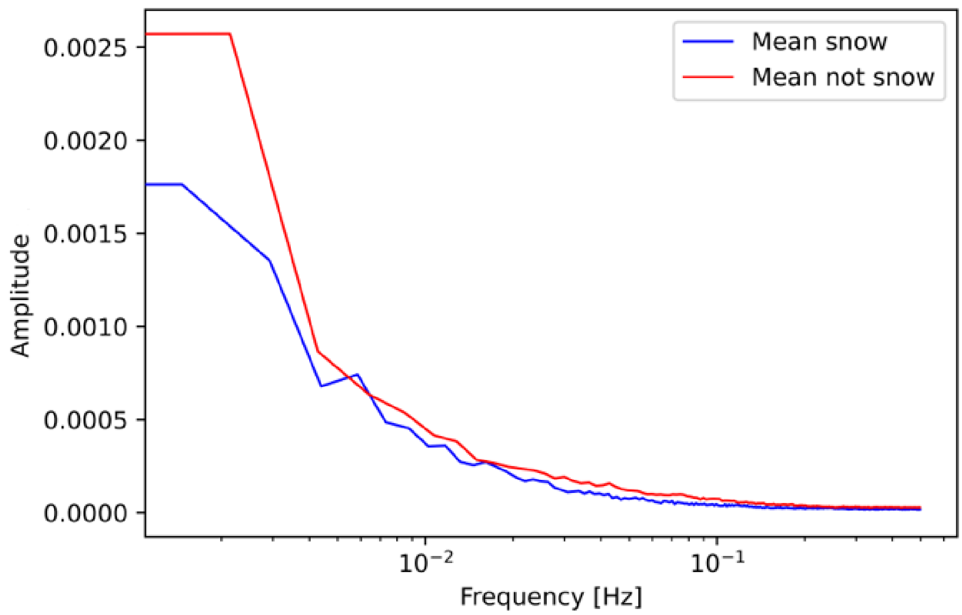

Figure 19. *Logarithmic representation of Mean Fourier Transform difference between snow and not snow passes*

4.2 LDA

Using the LDA with the STFT and the descriptive statistics, the accuracy score of the model was 0.6518.

Changing the LDA model to take in the segmented passes with the frequency information from the Fourier Transform and the descriptive statistics, the accuracy score of the model was 0.6208. When another descriptive statistic was added that gives the distance from the pass's maximum elevation to the segment's mean elevation, the LDA model's accuracy score changed to 0.6674.

Table 2 shows the impact of the different variables on the LDA model. The table shows the variable removed and what the model’s accuracy score became with the rest of the variables remaining.

Table 2. *Variables impact on the accuracy score when using the LDA with Fourier Transform*

Variable removed	Accuracy score
None	0.6674
Mean	0.6674

Median	0.6680
Variance	0.6687
Standard deviation	0.6708
Kurtosis	0.6708
Skewness	0.6742
Median elevation	0.6749
Distance from the median elevation of the segment to the max elevation of the pass	0.6208
Fourier Transform	0.6762

Using the matrix of variable combinations to determine which combinations give the best accuracy score, the top ten results are shown in Table 3.

Table 3. *Variables used for the LDA with Fourier Transform and the accuracy score*

Variables used	Accuracy score
Median, Variance, Standard deviation, Skewness, Distance from the median elevation of the segment to the max elevation of the pass	0.6879
Median, Variance, Standard deviation, Kurtosis, Skewness, Distance from the median elevation of the segment to the max elevation of the pass	0.6872
Mean, Variance, Standard deviation, Skewness, Distance from the median	0.6865

elevation of the segment to the max elevation of the pass	
Mean, Variance, Standard deviation, Kurtosis, Skewness, Distance from the median elevation of the segment to the max elevation of the pass	0.6865
Mean, Median, Variance, Standard deviation, Skewness, Distance from the median elevation of the segment to the max elevation of the pass	0.6858
Mean, Median, Variance, Standard deviation, Distance from the median elevation of the segment to the max elevation of the pass	0.6851
Mean, Median, Variance, Standard deviation, Kurtosis, Skewness, Distance from the median elevation of the segment to the max elevation of the pass	0.6851
Median, Variance, Standard deviation, Distance from the median elevation of the segment to the max elevation of the pass	0.6831
Median, Variance, Standard deviation, Kurtosis, Distance from the median elevation of the segment to the max elevation of the pass	0.6824

Mean, Variance, Standard deviation, Distance from the median elevation of the segment to the max elevation of the pass	0.6824

4.2.1 LDA with the highest elevation segment

The results from the last LDA model, where only the highest elevation segments were used, give the model an accuracy score of 0.8393. The results of changing the window size to see how the accuracy score of the LDA model changes is represented in Table 4.

Table 4. *Window size change for the accuracy score of the LDA with Fourier Transform only using the highest elevations*

Window size	Accuracy score
30	0.8125
40	0.8125
50	0.8393
60	0.8661
70	0.8214
80	0.7946
90	0.7768
100	0.8482
110	0.7500
120	0.7946
130	0.7232
140	0.6607

150	0.7143

The results of combining changing the window size and removing variables to see how the accuracy score changes are shown in Table 5.

Table 5. *Changing window size and removing variables to see the accuracy score for the LDA with Fourier Transform*

Removed variables / Window size	None	Mean	Median	Variance	Standard deviation	Kurtosis	Skewness	Median elevation	Fourier Transform
30	0.8125	0.8125	0.7946	0.8125	0.7768	0.7857	0.7946	0.7857	0.8125
40	0.8125	0.8125	0.8036	0.8125	0.8393	0.7946	0.8036	0.8036	0.8125
50	0.8393	0.8393	0.8393	0.8036	0.8304	0.8393	0.8306	0.8214	0.8393
60	0.8661	0.8661	0.8661	0.7946	0.8214	0.8393	0.8750	0.8661	0.8661
70	0.8214	0.8214	0.7946	0.8036	0.8214	0.8125	0.8214	0.8214	0.8214
80	0.7946	0.7946	0.7768	0.7768	0.7946	0.7946	0.7857	0.8036	0.7946
90	0.7768	0.7768	0.7946	0.7589	0.7500	0.7857	0.8125	0.7768	0.7768
100	0.8482	0.8482	0.8214	0.8125	0.8125	0.8482	0.8304	0.8482	0.8482
110	0.7500	0.7500	0.7500	0.7232	0.7857	0.7411	0.7768	0.7679	0.7500
120	0.7946	0.7946	0.7946	0.8036	0.7946	0.8036	0.8125	0.7946	0.7946
130	0.7232	0.7232	0.7232	0.7143	0.7232	0.7232	0.7143	0.7053	0.7232
140	0.6607	0.6607	0.6607	0.6964	0.6429	0.6607	0.6696	0.6339	0.6607
150	0.7143	0.7143	0.7232	0.7321	0.6964	0.7054	0.7143	0.6964	0.7143

The window size with the overall highest accuracy score was size 60. This window size is used further on in the analysis. The results from using the matrix of the variable variations to see what variable combinations give the LDA model the best accuracy are shown in Figure 20. For the variable variations corresponding to the accuracy scores, see appendix section A.

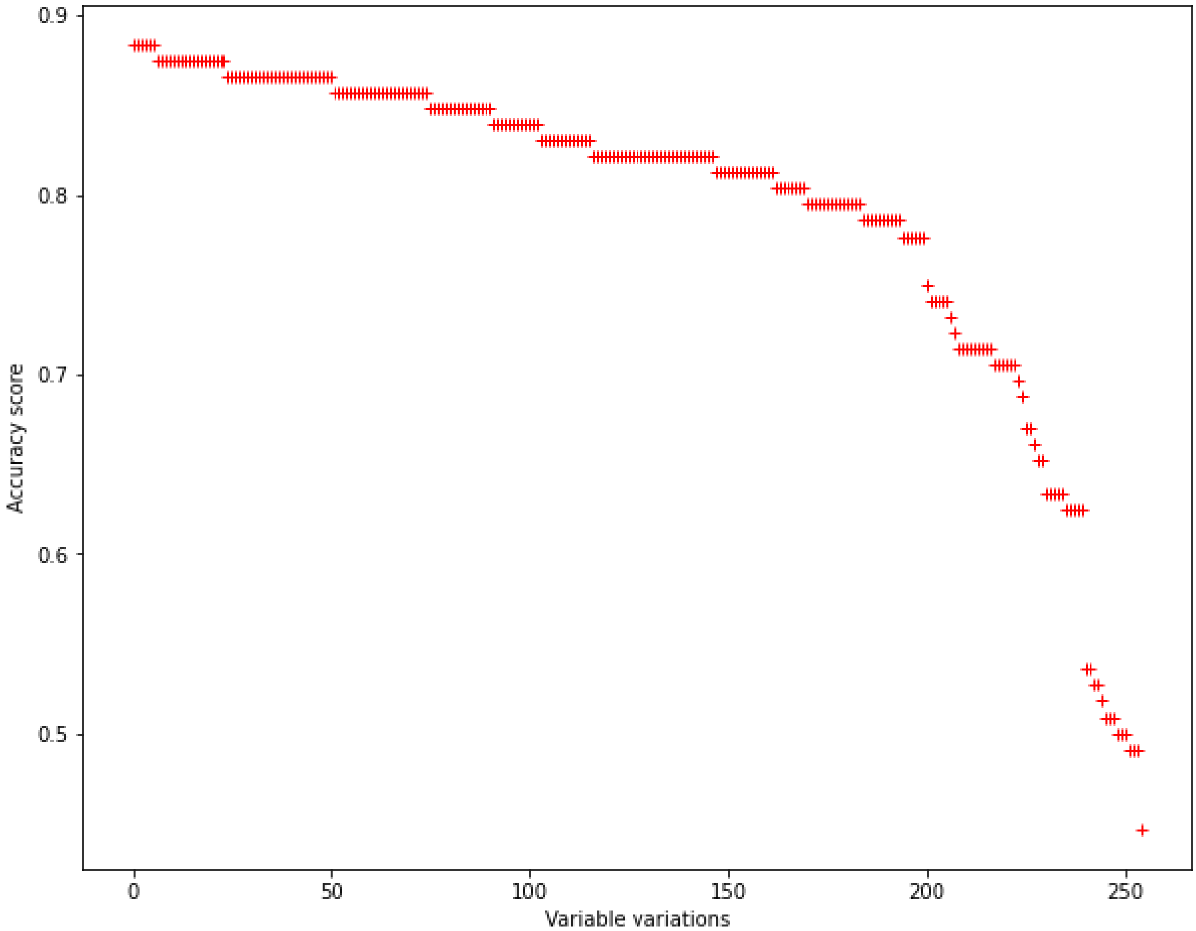

Figure 20. *Fourier Transform LDA windowsize 60 all variations of variables with the accuracy score*

The top 20 variable variations from the LDA model and the corresponding accuracy scores are represented in Table 6.

Table 6. *LDA top 20 variation of variables with highest elevation segment and window size 60 accuracy score*

Variables	Accuracy score
Mean, Median, Variance, Median elevation, Fourier Transform	0.8839

Mean, Variance, Standard deviation, Fourier Transform	0.8839
Mean, Variance, Standard deviation, Median elevation, Fourier Transform	0.8839
Median, Variance, Median elevation, Fourier Transform	0.8839
Variance, Standard deviation, Fourier Transform	0.8839
Variance, Standard deviation, Median elevation, Fourier Transform	0.8839
Mean, Median, Variance, Fourier Transform	0.8750
Mean, Median, Variance, Kurtosis, Fourier Transform	0.8750
Mean, Median, Variance, Standard deviation, Kurtosis, Fourier Transform	0.8750
Mean, Median, Variance, Standard deviation, Kurtosis, Median elevation, Fourier Transform	0.8750
Mean, Variance, Fourier Transform	0.8750
Mean, Variance, Kurtosis, Fourier Transform	0.8750
Mean, Variance, Median elevation, Fourier Transform	0.8750

Mean, Variance, Standard deviation, Kurtosis, Fourier Transform	0.8750
Mean, Variance, Standard deviation, Kurtosis, Median elevation, Fourier Transform	0.8750
Median, Variance, Fourier Transform	0.8750
Median, Variance, Kurtosis, Fourier Transform	0.8750
Median, Variance, Standard deviation, Kurtosis, Fourier Transform	0.8750
Median, Variance, Standard deviation, Kurtosis, Median elevation, Fourier Transform	0.8750
Variance, Fourier Transform	0.8750

The results from verifying the variables that give the highest accuracy score are shown in Figure 21 and Figure 22. Figure 22 also shows the mean of each variable variation as a dash.

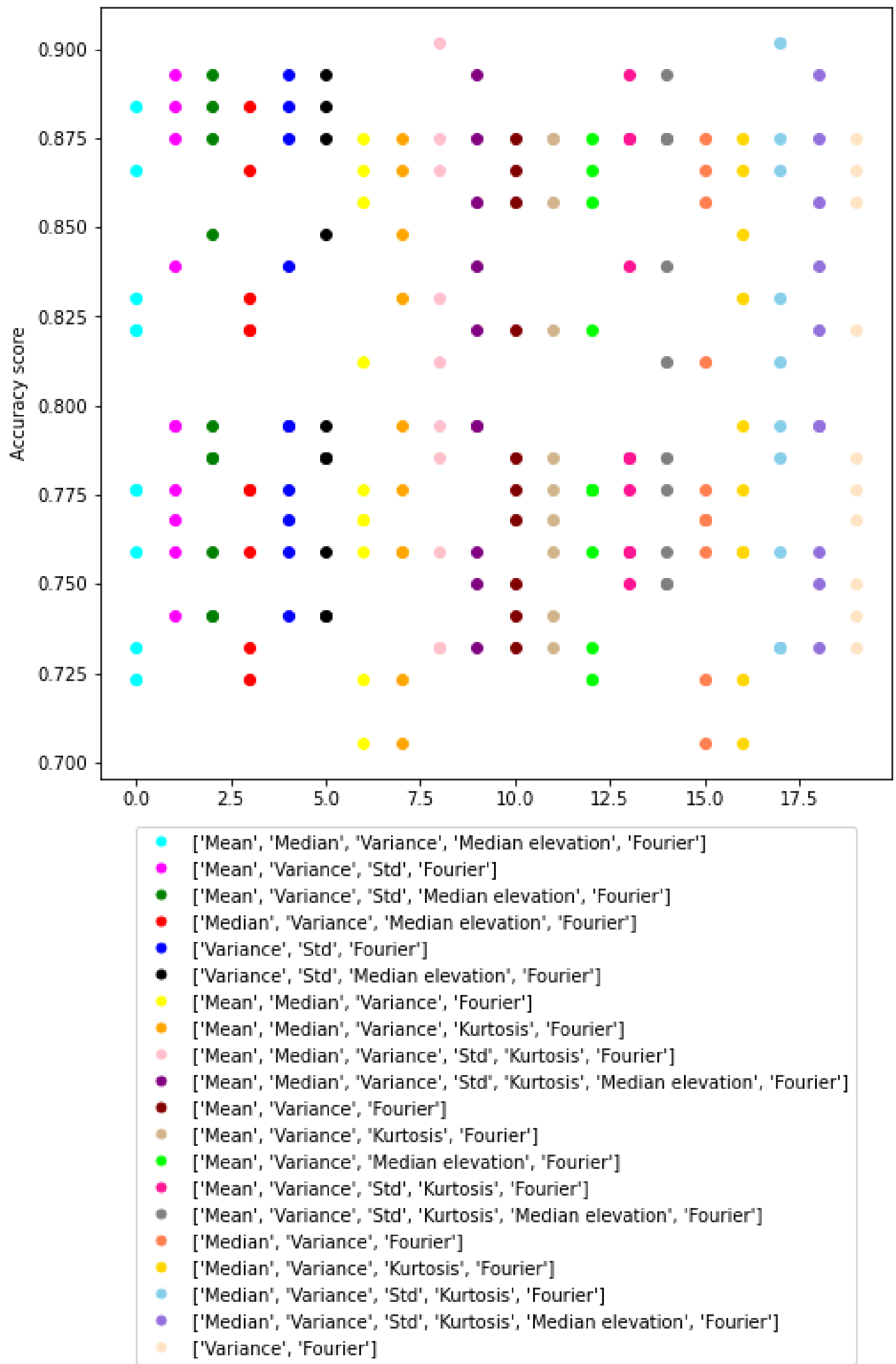

Figure 21. *LDA 10 train test split variations of the 20 top variable variations for the highest elevation window with size 60*

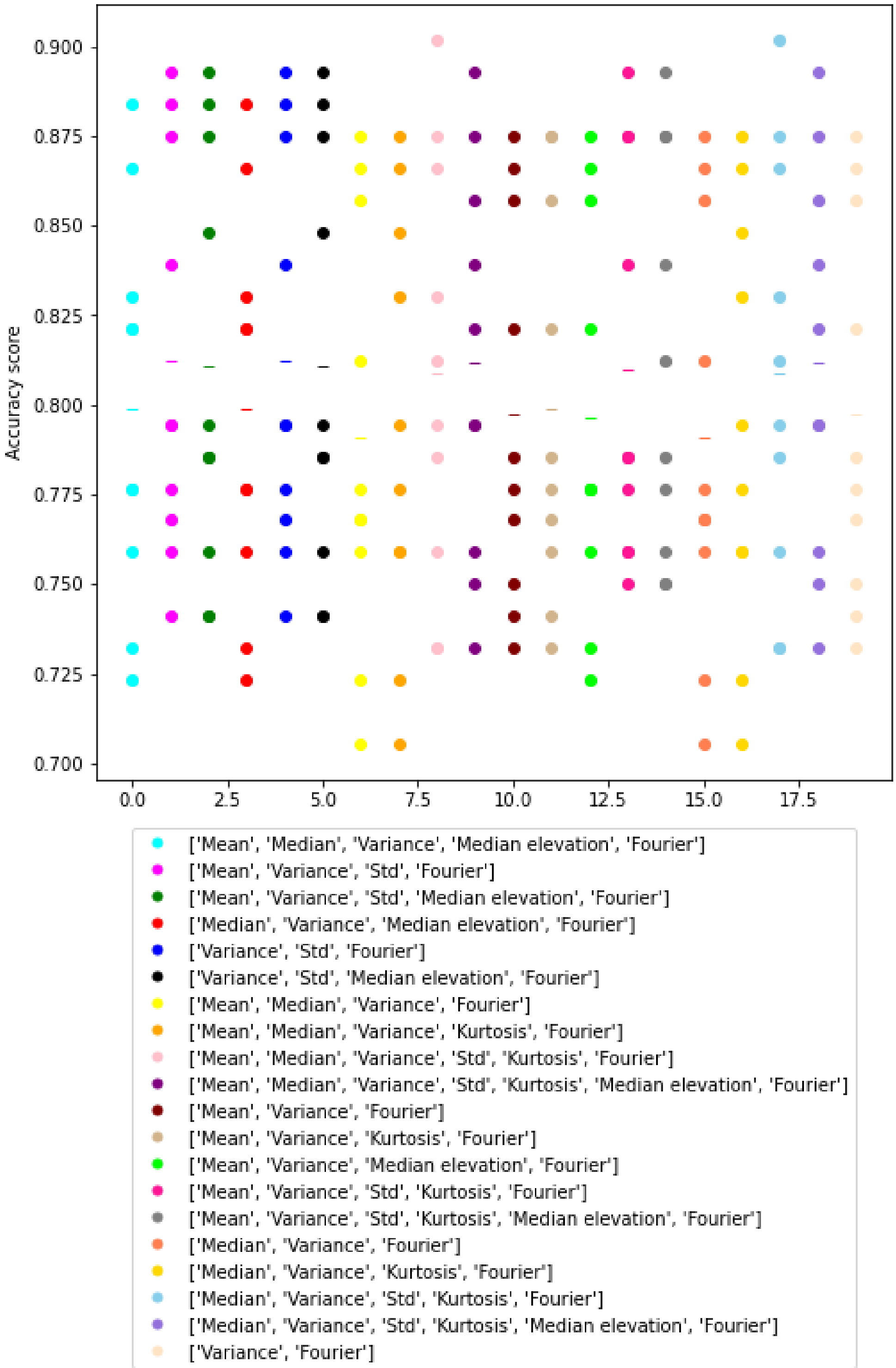

Figure 22. *LDA 10 train test split variations of the 20 top variable variations for the highest elevation window with size 60 including the mean of the samples*

A comparison of the means from each variable combinations are shown in Figure 23.

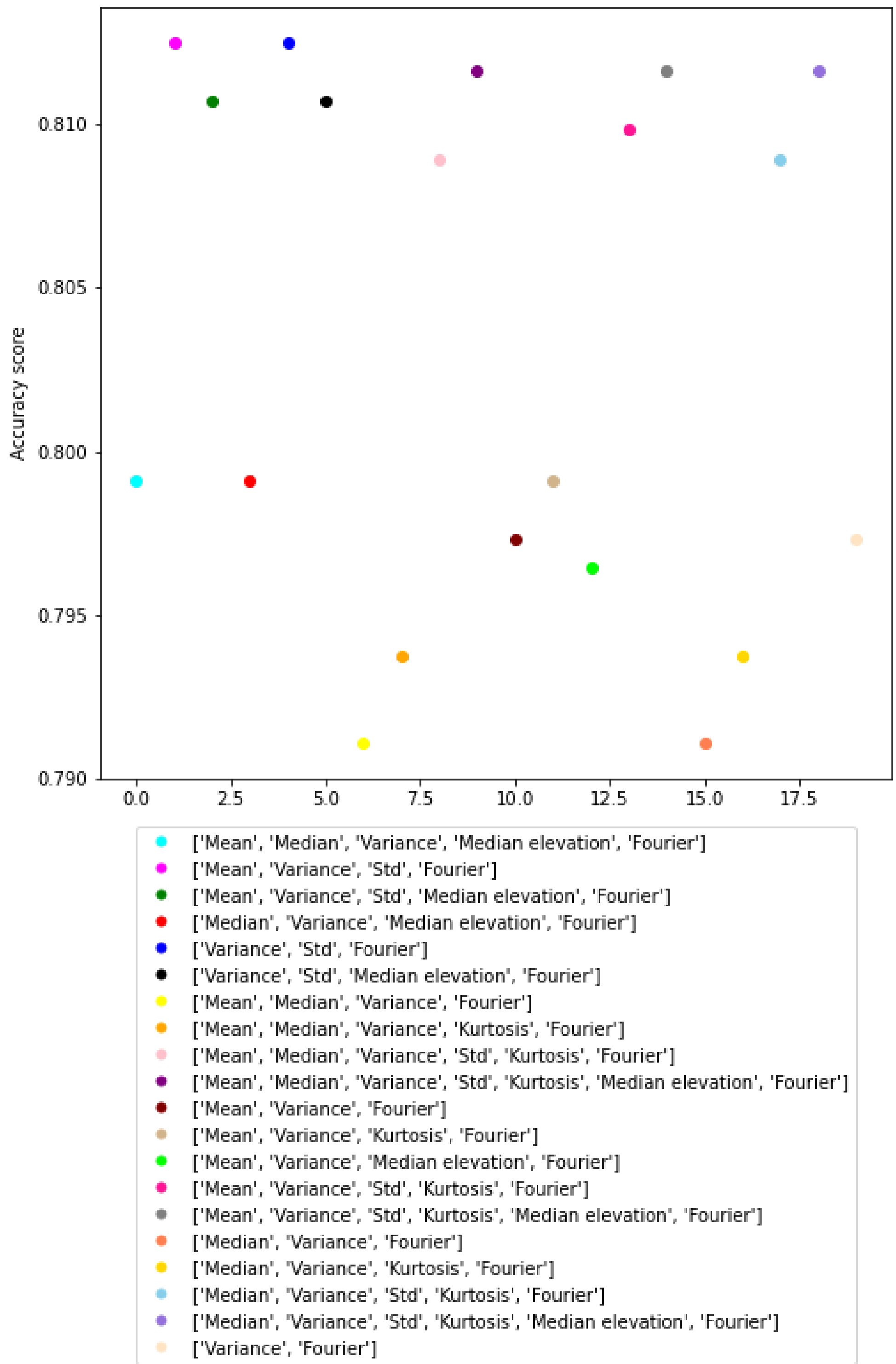

Figure 23. *LDA 10 train test split variations of the 20 top variable variations for the highest elevation window with size 60 only mean values*

The mean and variance within each of the variable variations are shown in Table 7.

***Table 7**. LDA 10 train test split variations of the 20 top variable variations for the highest elevation window with size 60 mean and variance*

Variables	Mean	Variance
Mean, Median, Variance, Median elevation, Fourier Transform	0.7991	0.0029
Mean, Variance, Standard deviation, Fourier Transform	0.8125	0.0031
Mean, Variance, Standard deviation, Median elevation, Fourier Transform	0.8107	0.0035
Median, Variance, Median elevation, Fourier Transform	0.7991	0.0029
Variance, Standard deviation, Fourier Transform	0.8125	0.0031
Variance, Standard deviation, Median elevation, Fourier Transform	0.8107	0.0035
Mean, Median, Variance, Fourier Transform	0.7911	0.0035
Mean, Median, Variance, Kurtosis, Fourier Transform	0.7938	0.0035
Mean, Median, Variance, Standard deviation, Kurtosis, Fourier Transform	0.8089	0.0035

Mean, Median, Variance, Standard deviation, Kurtosis, Median elevation, Fourier Transform	0.8116	0.0030
Mean, Variance, Fourier Transform	0.7973	0.0029
Mean, Variance, Kurtosis, Fourier Transform	0.7991	0.0029
Mean, Variance, Median elevation, Fourier Transform	0.7964	0.0030
Mean, Variance, Standard deviation, Kurtosis, Fourier Transform	0.8098	0.0030
Mean, Variance, Standard deviation, Kurtosis, Median elevation, Fourier Transform	0.8116	0.0031
Median, Variance, Fourier Transform	0.7911	0.0035
Median, Variance, Kurtosis, Fourier Transform	0.7938	0.0035
Median, Variance, Standard deviation, Kurtosis, Fourier Transform	0.8089	0.0035
Median, Variance, Standard deviation, Kurtosis, Median elevation, Fourier Transform	0.8116	0.0030

Variance, Fourier Transform	0.7973	0.0029

5 Discussion

5.1 Fourier Transform

Looking at the Fourier Transform analysis results, the differences in the frequency domain within the classes is larger than the difference between the means of the different classes; this can be seen in Figure 15, Figure 17 and Figure 19. The variance within each class is also the largest in the areas where the means are the most dissimilar, as seen in Figure 16, Figure 18 and Figure 19.

Looking at the results, the mean of each class is not a good representation of the classes. The difference between the classes is also only present in the frequencies with the highest inaccuracy between the mean and the data in the class. This means the mean value will not be suitable for separating the classes. The dataset used for the Fourier Transform is small and only gives a narrow picture of the representation of passes. The class with snow was also only a small percentage of the overall data, making the mean of that class less accurate than the other class.

The results from the frequency data show that the passes have a wide variety of frequency representations within the classes. This indicates that noise, oscillation, and other factors impact the frequency more than the snow.

What could be looked at further in the Fourier Transform is only looking at a smaller section of the pass to try and reduce the noise. The section that would be most interesting to use would be the part of the signal with the highest elevation, as the snow typically lays on the crown of the radome.

5.2 LDA

5.2.1 LDA with STFT

Using the LDA with frequency information risks information having to be left out as the length of the passes decides the size of the frequency information. When the passes are of varying lengths, the shortest pass will decide how long the frequency information can be. This will impact LDA using both the STFT and the Fourier Transform.

Looking at the result of the LDA with the STFT and the descriptive statistics, the accuracy score was low enough to say that the model is not good enough to be used as a reliable prediction model. Because the STFT only has a small portion of the frequency information implemented, it gets an incomplete picture of the data. The LDA model taking in the STFT data this way does not give good results, but if the STFT could be implemented into the LDA in a way that keeps all the information, the results could get better. The descriptive statistics used for the LDA model could also be changed to see how they impact the results. Another analysing tool that could be used with the STFT data is the Fourier Transform of either parts of the pass or the whole pass. A different analysing tool implemented with the STFT in the LDA could be the Wavelet Transform of the pass. Similar to the STFT, the Wavelet refers to the time domain when showing the frequency data. The difference between the Wavelet Transform and the STFT is that the STFT shows the data in the frequency and time domain, while the Wavelet shows the data with the scale of the Wavelet and time. The Wavelet is a chirp that is moved across the signal with different scales to locate how much of a wavelet is located at each area of the time axis.

Factors that could be changed to see how it impacted the accuracy score of the LDA model are the window size of the STFT, the overlapping between the windows and the windowing function used. Retaining all the frequency information from the STFT would give the LDA model a better overall image of the pass. This could be done by changing every pass to the same length, cutting all the passes to the shortest pass, or adding a signal strength with zero floor height before the signal to get all the signals to the length of the longest pass. The passes could also be cut to only look at the area with the highest elevation. Another solution would be to mirror the signal around the highest elevation for signals that only increase or decrease. Implementing the Fourier Transform or the Wavelet Transform in the LDA model would also need to solve the length issue.

5.2.2 LDA with Fourier Transform

Comparing the results of the LDA with the STFT and the descriptive statistics and the results from the LDA of the segmented passes with the frequency information from the Fourier

Transform and the descriptive statistics, the accuracy scores were around the same value. Segmenting the data gives each of the segments equally weight in the LDA model, even though only a few of the segments have any relevant information about whether there is snow on the radome or not. Each pass has about eight segments, and about one to two of those segments have information that tells if the radome has a snow load. The overweight of segments without relevant information affects the model's accuracy.

Adding the descriptive statistic of the distance between the highest elevation within the pass and the mean height of the segment increased the accuracy of the LDA model, making it more accurate than the LDA model using the STFT. This is probably due to the passes with higher pointing angles going through more of the radome area where snow typically lays.

The LDA model that gave the best accuracy score was the one only using the segments with the highest elevation. The accuracy score rose from below 70 % when looking at every segment to above 80% when using only the highest elevation segment. The probable reason behind the accuracy score increase is that the segment with the most relevant information, whether the radome has snow or not on it, is the segment with the highest elevation angle.

The best accuracy score given when adjusting the segments' window size was from the window size of 60 data points. Looking at Table 6, the highest accuracies were between 88.4% and 87.5%. These results point to this being the best LDA model, but due to the limited data size cannot be definitively said to be the best model. The best variables will vary with different datasets, even from the same antennas. Looking at the window size results in Table 5, the range of sizes with the best accuracy scores was between 50 and 70 data points wide, with the window size 100 also having a high accuracy score.

The verification shows how different datasets affect the accuracy scores of the top variable variations in the last LDA model. Because of the data size in this project, verification is important, as small changes in the data will significantly impact the results. Looking at Figure 21, the accuracy score of each of the models lies between 70% and 90%, depending on the input data. This shows that the models' accuracy score depends significantly on the input and testing data. Looking at Figure 23, the mean of each model ended up in the same range, between 79% and 81% accuracy. The conclusion that can be drawn from this is that each model with the different variable variations will make equally good prediction models.

Looking at other ways to verify the last LDA model, one way would be to look at both the variable combination and the window size together. Having several ways of splitting the data between the testing set and training set for each of the window sizes and each variable variation for each of the window sizes. Analysing Table 6 to see what variables are in commonality between the top variable variations. All the top results use the frequency information from the Fourier Transform and the variance, indicating they give information that helps distinguish between the classes. However, skewness is one variable not in any of the top variable variations, indicating that this variable makes the classes harder to differentiate between.

Other tools could be used to verify the results of the last LDA method. One of those is the confusion matrix. The confusion matrix looks at the labels and predicted labels of the LDA to identify the common misclassifications. The matrix shows the percentage of the True Negative (TN), True Positive (TP), False Positive (FP) and False Negative (FN). Another way to examine the models' predictions is to analyse sensitivity and specificity. The sensitivity (TPR) relates to the methods' ability to classify as one class correctly, and the specificity (TNR) tells the models' ability to classify as not the wrong class correctly. The formula for these uses the same measurements as the confusion matrix, where the formula for TPR is shown in (5.1), and the formula for the TNR is shown in (5.2).

$$\text{TPR}=\frac{TP}{TP+FN} \tag{5.1}$$

$$\text{TNR}=\frac{TN}{TN+FP}. \tag{5.2}$$

Looking at other ways to improve the LDA prediction model, one way would be to make the data put into the LDA when using the highest elevation segment uniform. This could be done by centring the segment around the highest elevation. This would cause issues with passes where the highest elevation point is at either of the ends. This could be resolved using half of the segment size on the part of the data with the highest elevation and mirroring it, allowing it to follow the same shape as the other segments from passes with the highest point in the middle. The LDA model can also take in unlabelled data and predict what data fits in what category. This could be used to see what classes the data easily separates into.

An alternative to the LDA is the Analysis of variance (ANOVA). (Miller, 1997) ANOVA is a collection of different statistical methods, mainly used to look at the results to see what methods give the best results. The ANOVA is another commonly used method, which tells if there is a way to differentiate between two datasets. This method could help compare the means of the Fourier Transform of the two classes.

There are other analysing tools than the Fourier Transform and the STFT that could be used in the LDA. One of these tools is the Wavelet Transform. Another alternative would be the Hilbert Transform. The Hilbert Transform transforms the signal by phase-shifting the angles of the components of the signal 90°. When using the FFT, it is most often used to get the minimum-phase response from the spectral analysis.

5.3 Further work

Looking beyond this project to both how to further improve the models and tools used and discussing other methods that will expand on the project topic. Based on the results from this project, none of the analysing tools or LDA models was found to give a highly accurate model for data prediction. However, the project found some ways of looking at the data that gave better results than others, indicating that those ways are useful to further build upon. The project also provides information on what to look at in the data to differentiate between the classes.

Because of the time limit of this project, only a smaller sample data set was used to evaluate the models. For further testing, a much larger dataset should be labelled to give a better model that can look at a broader range of passes. However, the size of the dataset used in this project was not big enough to give any definitive answers but rather pointed in the direction of tools and models that would be useful.

An analysis tool not discussed during this project that would be interesting to apply to the problem would be the degree of symmetry. The passes have a symmetrical aspect to both the signal strength without interference and symmetry with how the snow impacts the signals. The biggest challenge with symmetry is the noise that often occurs, especially when there is snow. If implemented, the symmetry could be used as a variable put into the LDA or with another method.

Looking beyond the data available for this project, historical weather data would be an interesting aspect to look at. The weather data could be used as a future predictor saying how likely the weather is to produce snow and ice on the radome. The prediction model not only looks at the snow already lying but also makes sure there is a warning before it happens.

The long-term goal of this project on KSAT's side would be to find a method that could, with high accuracy, predict the classification of the passes. Then, looking beyond this project's scope, the method could be used to create a database of classified data. This data could be used for a machine learning program that detects all abnormalities with the antenna to spacecraft communication.

6 Conclusion

This project used signal processing tools to look at signal strength and pointing angle of satellite antennas to try and detect snow and ice on radomes. The antennas used for this project are located in the arctic region. The radomes protect the antennas from the arctic climate, but during the winter months, the radomes often get a layer of snow or ice on the top, reducing the signal strength between antenna and satellite. The project aims to answer two questions: Can signal processing be used to detect snow and ice on the radomes, and what signal processing tools and methods give the best results.

Before the analysing tools were applied, the data were manually classified as eighter snow or no snow. The two main ways the data was analysed were the Fourier Transform and the LDA method. The Fourier Transform was used on the data to see if there is a way to distinguish between the classes based on the signal strength. The first LDA model used the STFT to see if the LDA could be used as a predictor for new data. The second LDA model looked at segmenting the passes into equally sized segments and using the segments and their frequency data using the Fourier Transform to train the LDA. The last LDA model was applied using only the segments containing the highest elevation within each pass.

The results looking solely at the Fourier Transform of the signal strength gave little information that could easily distinguish between the classes of snow or no snow. The LDA with STFT could place some of the passes within their correct classes but have low accuracy. Segmenting the data and using the LDA with the Fourier Transform gave about the same results as using the LDA with the STFT. However, using only the highest elevation segments from the passes gave better results than the previous LDA models. This is mainly because snow and ice builds-up at the highest elevations at the crown of the radome. Verifying the best results of the last LDA model gave an average of 80% accuracy when classifying the data.

The analysing tools and LDA models found with the best results can be further explored by adjusting the metrics and adding other variables to tell more about the passes that might help the model's accuracy. Beyond that, implementing weather data in conjunction with the signal strength could make a predictor for snow build-up in the future. The end goal for KSAT would be to eventually have a method that gives a high accuracy to create an extensive library of labelled data. This data can be used for a machine learning algorithm that can provide a complete picture of the state of the antenna.

Works cited

Alsberg, B. K., n.d. *Chemometrics.* s.l.:s.n.

Anon., 2022. *KSAT.* [Online]
Available at: http://www.ksat.no/no/about-us/
[Accessed 14 01 2022].

Bryne, C. L., 2005. *Signal Processing A Mathematical Approach.* 2nd red. s.l.:CRC Press.

Chantal Cappelletti, S. B. B. K. M., 2020. *CubeSat Handbook.* s.l.:Elsevier.

Elbert, B., 2008. *Introduction to Satellite Communication.* s.l.:Artech House.

Fisher, R. A., 1936. *The use of multiple measurements in taxonomic problems as an example of linear discriminant analysis,* s.l.: Annals of Eugenics.

Harris, F. J., 1987. Multirate FIR Filters for Interpolating and Desampling. In: *Handbook of Digital Signal Processing.* s.l.:Elsevier, pp. 173-287.

Ippolito Jr, L. J., 2008. *Satellite Communications Systems Engineering.* s.l.:WILEY.

Izenman, A. J., 2008. *Modern Multivariate Statistical Techniques.* s.l.:Springer.

Jaime F. Delgado Saa, M. S. G., 2010. EEG Signal Classification Using Power Spectral Features and linear Discriminant Analysis: A Brain Computer Interface Application. *laccei,* June.

Kozakoff, D. J., 2009. *Analysis of Radome Enclosed Antennas.* 2nd red. s.l.:Artech House.

Kreyszig, E., 2011. *Advanced Engineering Mathematics.* s.l.:WILEY.

Miller, Jr, R. G., 1997. *Beyond ANOVA: Basics of Applied Statistics.* First red. s.l.:Chapmann & Hall/CRC.

Petros Xanthopoulos, P. M. P. T. B. T., 2013. *Robust Data Mining.* s.l.:Springer.

Portnoff, M. R., 1980. Time-Frequency Representation of Digital Signals and Systems Based on Short-Time Fourier Analysis. *IEEE*, February.

Qi, Y., 2021. Accurate diagnosis of lung tissues for 2D Raman spectrogram by deep learning based on short-time Fourier transform. *Sciencedirect*, June.

Sengur, A., 2007. An expert system based on linear discriminant analysis and adaptive neuro-fuzzy interference system to diagnosis heart valve disease. *Sciencedirect*, June.

W.T Cochran, J. C., 1967. What is the fast Fourier transform?. *IEEE*, October.

Yonggi Hong, Y. Y. J. P., 2021. Linear Discriminant Analysis-Based Motion Classification Using Distributed Micro Doppler Radars with Limited Backhaul. *ncbi*, April.

Appendix

A Table

This table shows variables used and the corresponding accuracy score from Figure 20.

Variables used	Accuracy score
Mean, Median, Variance, Median elevation, Fourier Transform	0.8839
Mean, Variance, Standard deviation, Fourier Transform	0.8839
Mean, Variance, Standard deviation, Median elevation, Fourier Transform	0.8839
Median, Variance, Median elevation, Fourier Transform	0.8839
Variance, Standard deviation, Fourier Transform	0.8839
Variance, Standard deviation, Median elevation, Fourier Transform	0.8839
Mean, Median, Variance, Fourier Transform	0.8750
Mean, Median, Variance, Kurtosis, Fourier Transform	0.8750
Mean, Median, Variance, Standard deviation, Kurtosis, Fourier Transform	0.8750
Mean, Median, Variance, Standard deviation, Kurtosis, Median elevation, Fourier Transform	0.8750

Mean, Variance, Fourier Transform	0.8750
Mean, Variance, Kurtosis, Fourier Transform	0.8750
Mean, Variance, Median elevation, Fourier Transform	0.8750
Mean, Variance, Standard deviation, Kurtosis, Fourier Transform	0.8750
Mean, Variance, Standard deviation, Kurtosis, Median elevation, Fourier Transform	0.8750
Median, Variance, Fourier Transform	0.8750
Median, Variance, Kurtosis, Fourier Transform	0.8750
Median, Variance, Standard deviation, Kurtosis, Fourier Transform	0.8750
Median, Variance, Standard deviation, Kurtosis, Median elevation, Fourier Transform	0.8750
Variance, Fourier Transform	0.8750
Variance, Kurtosis, Fourier Transform	0.8750
Variance, Median elevation, Fourier Transform	0.8750
Variance, Standard deviation, Kurtosis, Fourier Transform	0.8750

Variance, Standard deviation, Kurtosis, Median elevation, Fourier Transform	0.8750
Mean, Median, Variance, Kurtosis, Median elevation, Fourier Transform	0.8661
Mean, Median, Variance, Standard deviation	0.8661
Mean, Median, Variance, Standard deviation, Fourier Transform	0.8661
Mean, Median, Variance, Standard deviation, Kurtosis, Skewness, Fourier Transform	0.8661
Mean, Median, Variance, Standard deviation, Kurtosis, Skewness, Median elevation, Fourier Transform	0.8661
Mean, Median, Variance, Standard deviation, Median elevation	0.8661
Mean, Median, Variance, Standard deviation, Median elevation, Fourier Transform	0.8661
Mean, Variance	0.8661
Mean, Variance, Kurtosis, Median elevation, Fourier Transform	0.8661
Mean, Variance, Kurtosis, Skewness, Fourier Transform	0.8661

Mean, Variance, Standard deviation, Kurtosis, Skewness, Fourier Transform	0.8661
Mean, Variance, Standard deviation, Kurtosis, Skewness, Median elevation, Fourier Transform	0.8661
Mean, Variance, Standard deviation, Median elevation	0.8661
Median, Variance	0.8661
Median, Variance, Kurtosis, Median elevation, Fourier Transform	0.8661
Median, Variance, Standard deviation, Fourier Transform	0.8661
Median, Variance, Standard deviation, Kurtosis, Skewness, Fourier Transform	0.8661
Median, Variance, Standard deviation, Kurtosis, Skewness, Median elevation, Fourier Transform	0.8661
Median, Variance, Standard deviation, Median elevation	0.8661
Median, Variance, Standard deviation, Median elevation, Fourier Transform	0.8661
Variance, Kurtosis, Median elevation, Fourier Transform	0.8661
Variance, Kurtosis, Skewness, Fourier Transform	0.8661

Variance, Standard deviation	0.8661
Variance, Standard deviation, Kurtosis	0.8661
Variance, Standard deviation, Kurtosis, Skewness, Fourier Transform	0.8661
Variance, Standard deviation, Kurtosis, Skewness, Median elevation, Fourier Transform	0.8661
Variance, Standard deviation, Median elevation	0.8661
Mean, Median, Variance, Standard deviation, Kurtosis, Median elevation	0.8571
Mean, Median, Variance, Standard deviation, Kurtosis, Skewness	0.8571
Mean, Median, Variance, Standard deviation, Kurtosis, Skewness, Median elevation	0.8571
Mean, Median, Variance, Standard deviation, Skewness, Median elevation	0.8571
Mean, Standard deviation, Kurtosis, Median elevation	0.8571
Mean, Standard deviation, Median elevation	0.8571
Mean, Variance, Kurtosis, Skewness, Median elevation, Fourier Transform	0.8571
Mean, Variance, Standard deviation	0.8571

Mean, Variance, Standard deviation, Kurtosis	0.8571
Mean, Variance, Standard deviation, Kurtosis, Median elevation	0.8571
Mean, Variance, Standard deviation, Kurtosis, Skewness	0.8571
Mean, Variance, Standard deviation, Kurtosis, Skewness, Median elevation	0.8571
Median, Standard deviation, Kurtosis, Median elevation	0.8571
Median, Standard deviation, Median elevation	0.8571
Median, Variance, Standard deviation	0.8571
Median, Variance, Standard deviation, Kurtosis	0.8571
Median, Variance, Standard deviation, Kurtosis, Median elevation	0.8571
Median, Variance, Standard deviation, Kurtosis, Skewness	0.8571
Median, Variance, Standard deviation, Kurtosis, Skewness, Median elevation	0.8571
Variance, Kurtosis, Skewness, Median elevation, Fourier Transform	0.8571

Variance, Standard deviation, Kurtosis, Median elevation	0.8571
Variance, Standard deviation, Kurtosis, Skewness	0.8571
Variance, Standard deviation, Kurtosis, Skewness, Median elevation	0.8571
Variance, Standard deviation, Skewness	0.8571
Mean, Median, Standard deviation, Kurtosis, Median elevation	0.8482
Mean, Median, Variance, Standard deviation, Kurtosis	0.8482
Mean, Median, Variance, Standard deviation, Skewness	0.8482
Mean, Standard deviation	0.8482
Mean, Variance, Skewness, Fourier Transform	0.8482
Mean, Variance, Standard deviation, Skewness, Fourier Transform	0.8482
Mean, Variance, Standard deviation, Skewness, Median elevation	0.8482
Mean, Variance, Standard deviation, Skewness, Median elevation, Fourier Transform	0.8482
Median, Standard deviation	0.8482

Median, Variance, Standard deviation, Skewness, Median elevation	0.8482
Standard deviation	0.8482
Standard deviation, Median elevation	0.8482
Variance, Skewness, Fourier Transform	0.8482
Variance, Standard deviation, Skewness, Fourier Transform	0.8482
Variance, Standard deviation, Skewness, Median elevation	0.8482
Variance, Standard deviation, Skewness, Median elevation, Fourier Transform	0.8482
Mean, Median, Standard deviation	0.8393
Mean, Median, Standard deviation, Median elevation	0.8393
Mean, Median, Variance, Standard deviation, Skewness, Fourier Transform	0.8393
Mean, Median, Variance, Standard deviation, Skewness, Median elevation, Fourier Transform	0.8393
Mean, Variance, Skewness, Median elevation, Fourier Transform	0.8393
Mean, Variance, Standard deviation, Skewness	0.8393

Median, Variance, Standard deviation, Skewness	0.8393
Median, Variance, Standard deviation, Skewness, Fourier Transform	0.8393
Median, Variance, Standard deviation, Skewness, Median elevation, Fourier Transform	0.8393
Standard deviation, Kurtosis, Median elevation	0.8393
Variance	0.8393
Variance, Skewness, Median elevation, Fourier Transform	0.8393
Fourier Transform	0.8304
Mean, Fourier Transform	0.8304
Mean, Median, Standard deviation, Fourier Transform	0.8304
Mean, Median, Standard deviation, Kurtosis, Skewness, Median elevation	0.8304
Mean, Median, Standard deviation, Skewness, Fourier Transform	0.8304
Mean, Median, Standard deviation, Skewness, Median elevation	0.8304
Mean, Standard deviation, Kurtosis, Skewness, Median elevation	0.8304

Mean, Standard deviation, Skewness, Median elevation	0.8304
Median, Standard deviation, Fourier Transform	0.8304
Median, Standard deviation, Kurtosis, Skewness, Median elevation	0.8304
Median, Standard deviation, Skewness, Fourier Transform	0.8304
Median, Standard deviation, Skewness, Median elevation	0.8304
Standard deviation, Skewness, Median elevation	0.8304
Mean, Median, Fourier Transform	0.8214
Mean, Median, Kurtosis, Fourier Transform	0.8214
Mean, Median, Kurtosis, Median elevation, Fourier Transform	0.8214
Mean, Median, Median elevation, Fourier Transform	0.8214
Mean, Median, Standard deviation, Kurtosis, Fourier Transform	0.8214
Mean, Median, Standard deviation, Kurtosis, Median elevation, Fourier Transform	0.8214

Mean, Median, Standard deviation, Median elevation, Fourier Transform	0.8214
Mean, Median, Standard deviation, Skewness, Median elevation, Fourier Transform	0.8214
Mean, Median, Variance, Kurtosis, Skewness, Fourier Transform	0.8214
Mean, Median, Variance, Kurtosis, Skewness, Median elevation, Fourier Transform	0.8214
Mean, Median, Variance, Skewness, Fourier Transform	0.8214
Mean, Median, Variance, Skewness, Median elevation, Fourier Transform	0.8214
Mean, Standard deviation, Kurtosis	0.8214
Mean, Standard deviation, Kurtosis, Median elevation, Fourier Transform	0.8214
Mean, Standard deviation, Median elevation, Fourier Transform	0.8214
Median, Fourier Transform	0.8214
Median, Kurtosis, Fourier Transform	0.8214
Median, Kurtosis, Median elevation, Fourier Transform	0.8214

Median, Median elevation, Fourier Transform	0.8214
Median, Standard deviation, Kurtosis	0.8214
Median, Standard deviation, Kurtosis, Fourier Transform	0.8214
Median, Standard deviation, Kurtosis, Median elevation, Fourier Transform	0.8214
Median, Standard deviation, Median elevation, Fourier Transform	0.8214
Median, Standard deviation, Skewness, Median elevation, Fourier Transform	0.8214
Median, Variance, Kurtosis, Skewness, Fourier Transform	0.8214
Median, Variance, Kurtosis, Skewness, Median elevation, Fourier Transform	0.8214
Median, Variance, Skewness, Fourier Transform	0.8214
Median, Variance, Skewness, Median elevation, Fourier Transform	0.8214
Standard deviation, Kurtosis	0.8214
Standard deviation, Kurtosis, Median elevation, Fourier Transform	0.8214
Standard deviation, Median elevation, Fourier Transform	0.8214

Kurtosis, Fourier Transform	0.8125
Kurtosis, Median elevation, Fourier Transform	0.8125
Mean, Kurtosis, Fourier Transform	0.8125
Mean, Kurtosis, Median elevation, Fourier Transform	0.8125
Mean, Median, Standard deviation, Kurtosis	0.8125
Mean, Median, Standard deviation, Kurtosis, Skewness, Fourier Transform	0.8125
Mean, Median, Variance	0.8125
Mean, Median elevation, Fourier Transform	0.8125
Mean, Standard deviation, Fourier Transform	0.8125
Mean, Standard deviation, Kurtosis, Fourier Transform	0.8125
Median, Standard deviation, Kurtosis, Skewness, Fourier Transform	0.8125
Median elevation, Fourier Transform	0.8125
Standard deviation, Fourier Transform	0.8125
Standard deviation, Kurtosis, Fourier Transform	0.8125
Standard deviation, Kurtosis, Skewness, Median elevation	0.8125

Mean, Median, Skewness, Fourier Transform	0.8036
Mean, Skewness, Fourier Transform	0.8036
Mean, Standard deviation, Kurtosis, Skewness, Fourier Transform	0.8036
Mean, Standard deviation, Skewness, Fourier Transform	0.8036
Median, Skewness, Fourier Transform	0.8036
Skewness, Fourier Transform	0.8036
Standard deviation, Kurtosis, Skewness, Fourier Transform	0.8036
Standard deviation, Skewness, Fourier Transform	0.8036
Kurtosis, Skewness, Fourier Transform	0.7946
Mean, Kurtosis, Skewness, Fourier Transform	0.7946
Mean, Median, Kurtosis, Skewness, Fourier Transform	0.7946
Mean, Median, Standard deviation, Kurtosis, Skewness	0.7946
Mean, Median, Standard deviation, Kurtosis, Skewness, Median elevation, Fourier Transform	0.7946

Mean, Median, Standard deviation, Skewness	0.7946
Mean, Standard deviation, Kurtosis, Skewness	0.7946
Mean, Standard deviation, Kurtosis, Skewness, Median elevation, Fourier Transform	0.7946
Mean, Standard deviation, Skewness	0.7946
Median, Kurtosis, Skewness, Fourier Transform	0.7946
Median, Standard deviation, Kurtosis, Skewness	0.7946
Median, Standard deviation, Kurtosis, Skewness, Median elevation, Fourier Transform	0.7946
Median, Variance, Kurtosis	0.7946
Standard deviation, Kurtosis, Skewness, Median elevation, Fourier Transform	0.7946
Mean, Median, Skewness, Median elevation, Fourier Transform	0.7857
Mean, Skewness, Median elevation, Fourier Transform	0.7857
Mean, Standard deviation, Skewness, Median elevation, Fourier Transform	0.7857

Mean, Variance, Kurtosis	0.7857
Median, Skewness, Median elevation, Fourier Transform	0.7857
Median, Standard deviation, Skewness	0.7857
Skewness, Median elevation, Fourier Transform	0.7857
Standard deviation, Kurtosis, Skewness	0.7857
Standard deviation, Skewness, Median elevation, Fourier Transform	0.7857
Variance, Kurtosis	0.7857
Kurtosis, Skewness, Median elevation, Fourier Transform	0.7768
Mean, Kurtosis, Skewness, Median elevation, Fourier Transform	0.7768
Mean, Median, Kurtosis, Skewness, Median elevation, Fourier Transform	0.7768
Mean, Median, Variance, Kurtosis	0.7768
Median, Kurtosis, Skewness, Median elevation, Fourier Transform	0.7768
Standard deviation, Skewness	0.7768
Variance, Median elevation	0.7500
Mean, Median, Variance, Skewness, Median elevation	0.7411

Mean, Variance, Skewness, Median elevation	0.7411
Median, Variance, Skewness, Median elevation	0.7411
Variance, Kurtosis, Median elevation	0.7411
Variance, Skewness, Median elevation	0.7411
Mean, Variance, Median elevation	0.7321
Median, Variance, Median elevation	0.7232
Mean, Median, Variance, Kurtosis, Skewness, Median elevation	0.7143
Mean, Median, Variance, Median elevation	0.7143
Mean, Variance, Kurtosis, Median elevation	0.7143
Mean, Variance, Kurtosis, Skewness	0.7143
Median, Variance, Kurtosis, Median elevation	0.7143
Median, Variance, Kurtosis, Skewness	0.7143
Variance, Kurtosis, Skewness	0.7143
Variance, Kurtosis, Skewness, Median elevation	0.7143
Variance, Skewness	0.7143
Mean, Median, Variance, Kurtosis, Skewness	0.7054

Mean, Median, Variance, Skewness	0.7054
Mean, Variance, Kurtosis, Skewness, Median elevation	0.7054
Mean, Variance, Skewness	0.7054
Median, Variance, Kurtosis, Skewness, Median elevation	0.7054
Median, Variance, Skewness	0.7054
Mean, Median, Variance, Kurtosis, Median elevation	0.6964
Mean, Median, Kurtosis, Skewness, Median elevation	0.6875
Kurtosis, Median elevation	0.6696
Mean, Median, Median elevation	0.6696
Mean, Median, Skewness, Median elevation	0.6607
Kurtosis, Skewness, Median elevation	0.6518
Median elevation	0.6518
Mean, Kurtosis, Median elevation	0.6339
Mean, Median, Kurtosis, Median elevation	0.6339
Mean, Median elevation	0.6339
Median, Kurtosis, Median elevation	0.6339
Median, Median elevation	0.6339

Mean, Kurtosis, Skewness, Median elevation	0.6250
Mean, Skewness, Median elevation	0.6250
Median, Kurtosis, Skewness, Median elevation	0.6250
Median, Skewness, Median elevation	0.6250
Skewness, Median elevation	0.6250
Mean, Median, Kurtosis, Skewness	0.5357
Mean, Median, Skewness	0.5357
Mean, Skewness	0.5268
Median, Skewness	0.5268
Mean, Median, Kurtosis	0.5179
Mean, Kurtosis	0.5089
Mean, Kurtosis, Skewness	0.5089
Skewness	0.5089
Kurtosis, Skewness	0.5000
Median, Kurtosis	0.5000
Median, Kurtosis, Skewness	0.5000
Mean	0.4911
Mean, Median	0.4911

Median	0.4911
Kurtosis	0.4464